Durham E-Theses

Semi-Analytic Ground State Solutions of Two-Component Bose-Einstein Condensate in Two Dimensions

SRIDHAR, SWATI

How to cite:

SRIDHAR, SWATI (2014) *Semi-Analytic Ground State Solutions of Two-Component Bose-Einstein Condensate in Two Dimensions*, Durham theses, Durham University. Available at Durham E-Theses Online: http://etheses.dur.ac.uk/10955/

Semi-Analytic Ground State Solutions of Two-Component Bose-Einstein Condensate in Two Dimensions

by

Swati Sridhar

A thesis submitted in complete fulfilment of the requirements for the degree of

Masters by Research

Department of Physics
Durham University
September 2014

Abstract

In this thesis we study a two-component Bose-Einstein Condensate system in 2D, using a combination of approximate analytical and exact numerical methods of solving the Gross-Pitaevskii equation (GPE). We discuss some of the ways of finding approximate ground state solutions to the GPE, one of them being the Thomas-Fermi approximation. Using the Thomas-Fermi approximation, one can separate the system into two regimes; one where both components are disks and one where one of the components is a disk and the other component is an annulus. However, the Thomas-Fermi approximation does not hold true beyond a critical value.

We demonstrate a method using which one can get more precise solutions for the GPE. This involves using a method of approximation of the GPE near the critical boundaries, which has been previously used for a single component Bose gas. This can be adapted for a two-component system in order obtain explicit solutions for a BEC in a 2D harmonic trap with repulsive interactions. We show in detail how this approximation works for the different regimes suggested by the Thomas-Fermi analysis and also for more generalized cases where one has different masses, particle numbers and trapping frequencies for the two components. This thesis also talks about how one could analyse the system using this approximation in 1D and 3D, shedding more light on what might be the parameters affecting the precision of the solution.

Acknowledgements

First and foremost I would like to thank my supervisor, Prof. Simon Gardiner for believing in me and giving me this opportunity to study in a field that I am passionate about, and for encouraging and guiding me throughout the course of this degree. It has certainly been a challenging yet immensely gratifying experience.

I would like to thank Dr. Peter Mason, Dr. Tom Billam, and Juan Polo for the timely help and advice. I would also like to thank my parents for all the love and support and my friends for making each day a happy memory.

Contents

Introduction

Bose-Einstein Condensate

A Bose-Einstein condensate (BEC) is a state of matter of dilute bosonic gas when cooled down to near absolute zero temperatures. Matter in this state can be treated as a single quantum mechanical entity which can be described by one wave function [1, 2]. It was first predicted by Albert Einstein in 1925 [3] based on the statistical formulation on the quantization of bosons by Satyendra Nath Bose [4]. The interest first developed in this because the idea behind a BEC implied displaying quantum behaviour on a macroscopic scale.

Bosons follow Bose-Einstein statistics which describe the statistical distribution of identical particles with integer spin. Unlike bosons, fermions have half integer spin and follow Fermi-Dirac statistics. In accordance with the Pauli exclusion principle, no two fermions with all the same quantum numbers are allowed to occupy the same quantum state. This does not hold true in the case of bosons, where there is no statistical limit on the number of bosons that are allowed to occupy the same energy state. The Bose-Einstein statistics predicts that a collection of non-interacting indistinguishable particles can occupy a set of available energy states such that a large fraction of the atoms would go into the lowest energy quantum state at very low but finite temper-

ature [3, 4]. When dilute gases of bosons are cooled down to very low temperatures, it causes the atoms to condense to the lowest quantum state, resulting in a new form of matter called a Bose-Einstein condensate. The critical temperature, (T_C), is the highest temperature below which a macroscopic proportion of particles will occupy the lowest possible energy state. According to Einstein, "A phase separation is effected; one part condensate, the rest remains a 'saturated ideal gas' " [3]. This phenomenon is known as Bose-Einstein condensation. The condition for this condensation to occur is that the phase space density must be greater than approximately unity, in units of $\hbar^{-3}$.

If one considers an ideal gas of particles with no interactions in different momentum states and given that the number of particles is less than the number of thermally accessible states, the particles will be in different states for high temperature and low density regimes. The gas behaves as a classical gas in this limit. However, as the temperature decreases or density increases, the number of states accessible per atom become smaller, forcing more particles into a single state. Any particle added from then on goes to the ground state [1–3].

BECs and Superfluids

A state of matter which is strongly connected to BECs is superfluidity. It is a state of matter which behaves like an ideal fluid with no viscosity and no entropy [5]. Superfluidity was first observed in liquid ^{4}He [1, 2]. Bose–Einstein condensation is the most fundamental physical mechanism accountable for the superfluid state in ^{4}He. In any normal gas, as the temperature reduces, the thermal de Broglie wavelength increases. The wavelength is such that it is generally considerably smaller than the

average inter-atomic separation, d. When this wavelength becomes equal to d, the bosons undergo a phase transition. This parallels to momentum phase condensation. The temperature at which this occurs is known as the critical temperature or the lambda temperature. The property of behaving as a superfluid can be observed in ^{4}He below $T_\lambda = 2.17K$. 100% of the liquid behaves as a superfluid for temperatures $T \to 0$. In the case of an ideal Bose gas, all of the particles condense into the lowest available energy state as $T \to 0$. However, an ideal Bose gas does not become a superfluid. And in liquid ^{4}He, only a small fraction of the atoms form a condensate although all of the atoms can flow without viscosity.

Although BEC and superfluids share the same underlying mechanism arising from macroscopic occupation of a single quantum state, the properties of a BEC in a gas are quite distinct and hence interesting to study. BEC is far more dilute and weakly interacting in comparison to superfluids. There is a subtle connection between a Bose-Einstein condensed system and a superfluid system. A BEC system may not necessarily exhibit superfluidity and lower dimensional systems may exhibit superfluid behaviour in the absence of a true condensate [1, 2, 6]. Finally, BEC is a ground state property whereas superfluidity is a property of the excited states.

Applications and experimental investigation

BEC of a dilute atomic gas was first realized in the laboratory by Eric Cornell and Carl Wieman in 1995 [7], by cooling a dilute vapour consisting of rubidium-87 atoms using a combination of laser cooling and magnetic evaporative cooling. Since then, it has been experimentally made using dilute gases, for example, rubidium, sodium,

lithium, potassium, hydrogen, metastable helium [8–13], etc.

BECs exhibit a wide range of macroscopic quantum phenomena, making them a topic of interest to study experimentally and theoretically. In recent years, it has become possible to realize mixtures of BECs with different internal states, and also different species [12, 14, 15]. The multicomponent quantum gases offer interacting quantum fields with a wide variety of physical scenarios. It has been observed that there can be spatial separation of the mixtures depending on the relative interaction strengths within each condensate and between the components as well. One gets different regimes based on these interaction strength values, as well as other parameters such as particle number, frequency of the harmonic oscillator potential and mass of the condensate components. It is interesting to study which parameters affect the system to a great extent and which have a more minimalistic effect on the system.

The equation describing the behaviour of the wave function of a BEC is the Gross-Pitaevskii equation (GPE). The GPE is a non-linear Schrödinger equation, which gives the condensate in the form of a single wave function. The theory behind describing a single-component BEC can be extended to systems where one or more quantum states are macroscopically occupied. One such example of a multi-component system is a mixture of two different species of bosons [14, 16], which can be two different atoms or two different isotopes of the same element. The first condensate mixture was realized by the JILA group using ^{87}Rb atoms with different hyperfine states [17]. One of the ways of determining the ground states include the Thomas-Fermi approximation and variational methods. A feature of the Thomas-Fermi is that it provides nearly exact solutions of the GPE in the limit of strong interactions. This thesis concerns itself with the two-component Thomas-Fermi solutions, and corrections to these solutions.

Chapter 1

Gross-Pitaevskii equation

1.1 Overview

This chapter discusses the Gross-Pitaevskii equation (GPE), which describes the interaction of nonuniform Bose gases, and the Bogoliubov approximation. The GPE gives the ground state of a system of identical bosons, using the mean-field approximation. A Bose gas can be described in terms of a field operator, $\hat{\psi}(r,t)$, in the Heisenberg picture by [1]

$$i\hbar\frac{d}{dt}\hat{\psi}(r,t) = [\hat{\psi}(r,t),\hat{H}] = \left[-\frac{\hbar^2\nabla^2}{2m} + V_{\text{ext}} + \int \hat{\psi}^\dagger(r',t)V(r'-r)\hat{\psi}(r',t)\,dr'\right]\hat{\psi}(r,t).$$

(1.1)

This is the Heisenberg equation of motion, where V_{ext} is the external potential. In the case of a condensate with a large number of particles, the quantum field operator in this equation can be replaced with a classical field, $\psi_{(}r,t)$, also called the order parameter or wave function of the condensate. This can be deduced from the Bogoliubov approximation for the lowest order at low temperatures [1]. Assuming that the classical field

varies slowly on distances of the order of the range of the interatomic forces one can obtain the equation

$$i\hbar\frac{\partial}{\partial t}\psi(r,t) = \left(-\frac{\hbar^2\nabla^2}{2m} + V_{\text{ext}}(r,t) + U_0|\psi(r,t)|^2\right)\psi(r,t)$$ (1.2)

for the order parameter with $U_0 = \int V_{\text{eff}}(r)dr = 4\pi\hbar^2 a_s/m$ [1], where a_s is the s-wave scattering length, m is the mass of the condensate and V_{eff} is the effective potential.

1.2   Single-component BEC

1.2.1   Basic Classical Equations

The Gross-Pitaevskii equation is a non-linear Schrödinger equation describing the properties of non-uniform Bose gas at zero-temperature, when the scattering length a_s is much less than the mean inter particle spacing. We adopt a mean-field approach, assuming that the wave function is the symmetrized product of a single particle wave function [2]. Therefore implying that all bosons are in the same quantum state, $\psi(r)$. In this mean-field regime, the classical energy functional for a single component BEC in a harmonic-oscillator potential is given as,

$$E = \int \psi^*(r)\left[-\frac{\hbar^2\nabla^2}{2m} + V(r) + \frac{U_0}{2}|\psi(r)|^2\right]\psi(r)\,dr,$$ (1.3)

where

$$V(r) = \frac{1}{2}m\omega^2 r^2$$ (1.4)

is the effective potential (= V_{eff}). In order to obtain the optimized ψ, we minimize the energy with respect to independent variations of $\psi(r)$ and its complex conjugate $\psi^*(r)$ subject to the condition that the total number of particles, N, be constant.

$$N = \int |\psi(r)|^2 \, d^2r. \tag{1.5}$$

One can write $\delta E - \mu \delta N = 0$, where the chemical potential μ is a Lagrange multiplier [2]. Equating to zero, the variation of $E - \mu N$ with respect to $\psi^*(r)$ gives

$$-\frac{\hbar^2}{2m}\nabla^2\psi(r) + V(r)\psi(r) + U_0|\psi(r)|^2\psi(r) = \mu\psi(r), \tag{1.6}$$

which is the time-independent GPE. The time-dependent GPE can be determined by Hamilton's equations of motion (where E describes a classical Hamiltonian field). On imposing the stationary conditon [1]

$$\delta\left[-i\hbar \int \psi_0^* \frac{\partial}{\partial t}\psi_0 \, drdt + \int E \, dt\right] = 0. \tag{1.7}$$

Using the following identity,

$$i\hbar\frac{\partial\psi_0(r,t)}{\partial t} = \frac{\delta E}{\delta\psi_0^*(r,t)}, \tag{1.8}$$

one obtains the time-dependent GPE as

$$i\hbar\frac{\partial\psi(r,t)}{\partial t} = \left(-\frac{\hbar^2}{2m}\nabla^2 + V(r) + U_0|\psi(r,t)|^2\right)\psi(r,t). \tag{1.9}$$

1.2.2 Linearized Excitations

In order to determine the condition that governs the stability of a two-component system, it is good to find the dispersion relation, highlighting the essential parameters. The dispersion relation that we find aids in knowing if some of these linearized excitations may become unstable beyond a certain critical point. One of the ways with which one can determine approximate steady-state solutions of the corresponding GPE is by linearizing it using the Bogoliubov transformation which diagonalize the Hamiltonians [Eq. (1.1)]. It is a good method to find stable, independent low-energy excitations. This method is equivalent to linearising the GPE by writing the order parameter of the form,

$$\psi_0(r,t) = \psi'(r,t)e^{-i\mu t/\hbar} = [\psi(r) + \vartheta(r,t)]e^{-i\mu t/\hbar}, \qquad (1.10)$$

where ϑ is a small quantity and μ is the chemical potential. This gives the linearized solution of the form

$$\vartheta(r,t) = \sum_i [u_i(r)e^{-i\omega_i t} + v_i^*(r)e^{-i\omega_i t}], \qquad (1.11)$$

where ω_i is the frequency of the oscillation. The functions $u_i(r)$ and $v_i(r)$ are the analogues of the Bogoliubov parameters and are the amplitudes of the system [1] for the non-uniform problem. For $\psi(r,t) = e^{-i\mu t/\hbar}[\psi(r)e^{-i\omega t} + v_i^* e^{i\omega t}]$, two linearized equations are obtained (Bogoliubov transformation) where, $n_0 = |\psi(r)|^2$ is the mean-field density. They are determined by solving the Gross-Pitaevskii equation in the linear limit by comparing the terms which involve a factor of $e^{-i\omega_i t/\hbar}$ and $e^{i\omega_i t/\hbar}$, respectively. For

8

the case where the trapping potential, V, is considered to be zero, one finds the solutions

$$u(r) = ue^{ik.r}, \tag{1.12}$$

$$v(r) = ve^{ik.r}, \tag{1.13}$$

using which the following pair of linear equations are obtained:

$$\hbar\omega u = \frac{\hbar^2 k^2}{2m}u + U_0 n_0(u + v), \quad \hbar\omega v = -\frac{\hbar^2 k^2}{2m}v + U_0 n_0(u + v), \tag{1.14}$$

which gives the analytic solution,

$$(\hbar\omega)^2 = \left(\frac{\hbar^2 k^2}{2m}\right)^2 + \frac{\hbar^2 k^2}{m}U_0 n, \tag{1.15}$$

for the frequency as a function of the wave number, k. One can choose the units such that $\hbar = m = U_0 n_0$, with the rescaled equation for the dispersion relation as

$$\omega^2 = k^2\left(\frac{k^2}{4} + 1\right). \tag{1.16}$$

This equation gives the Bogoliubov dispersion for a single component [Fig. 1.1]. From the energy spectrum or the Bogoliubov excitation spectrum one can infer that the weakly-interacting Bose gas satisfies the Landau criterion for superfluidity [1, 2]. The velocity of sound gives the critical velocity for a Bose gas to turn into a superfluid. The Landau velocity or the critical velocity is found as the line of minimum slope which intersects the dispersion relation graph. It can be used to predict the breakdown of superfluidity as an object moves through the BEC. It is to show how factors which
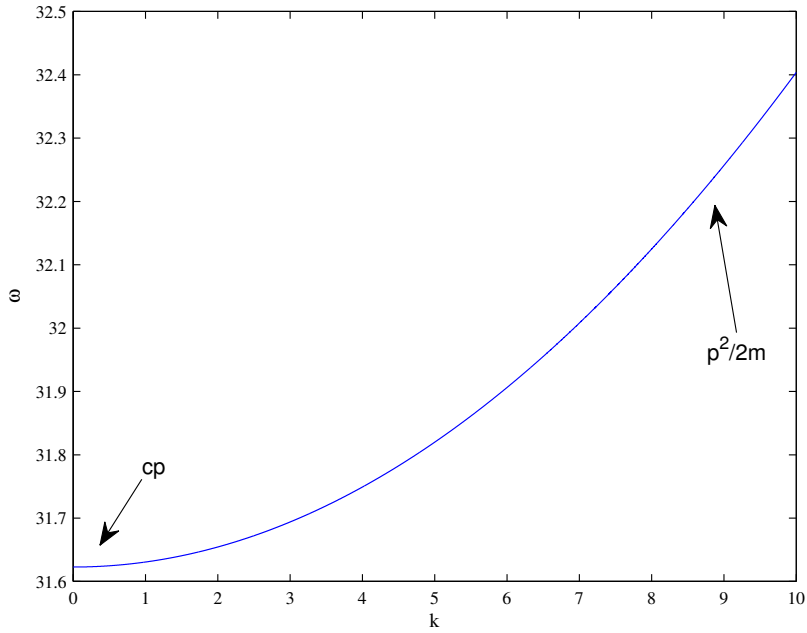
Figure 1.1: Dispersion relation for a single component BEC showing low and high excitations where c is the speed of light in vacuum and p is the momentum of the excitation, with $\hbar = m = U_0 n_0 = 1$.

have a negligible contribution, increase exponentially, i.e get magnified and are no longer negligible. It helps understand the character of the wave motion wherein, $\hbar\omega$ is the energy of an excitation characterized by the wave number, k [18].

1.3 Two-component BEC in 2D

In this section we extend the method of finding the dispersion spectrum for one component BEC to systems in which two-component condensate mixtures in 2D. The two-component Bose-Einstein condensate at zero temperature in the mean-field regime can be described in terms of two order parameters, i.e, the two wave functions, ψ_1 and ψ_2. These represent component 1 and component 2 respectively. The Gross-Pitaevskii energy functional of a stationary two-component, two dimensional BEC is given by

$$E[\psi_1, \psi_2] = \int \left\{ \sum_{k=1,2} \left[\frac{\hbar^2}{2m_k} |\nabla \psi_k|^2 + V_k(r)|\psi_k|^2 + \frac{U_k}{2}|\psi_k|^4 \right] + U_{12}|\psi_1|^2|\psi_2|^2 \right\} d^2r, \quad (1.17)$$

where $r^2 = x^2 + y^2$. The energy functional contains three interaction constants, namely, U_1 and U_2, which represent the internal interactions in a particular component, and U_{12} which represents the interactions between the two components. The intracomponent coupling strength is defined as $U_k = \sqrt{8\pi}\hbar^2 a_k/[m_k a_{zk}](k = 1, 2)$ and the intercomponent strength as $U_{12} = \sqrt{2\pi}\hbar^2 a_{12}/[m_{12} a_z]$, with reduced mass $m_{12}^{-1} = m_1^{-1} + m_2^{-1}$. The s-wave scattering lengths are a_k and a_{12}, and a_{zk} is the characteristic length of the harmonic oscillator in the z-direction, that is $a_{zk} = \sqrt{\hbar/m_k \omega_{zk}}$, with ω_{z1} and ω_{z2} the frequencies of the restriction in the z-direction. $a_z = (a_{z1} + a_{z2})/2$, is the average of the characteristic lengths of the harmonic oscillator in the z-direction [1, 19]. For the two-component coupled BEC the GPE can be written as [14, 20]:

$$i\hbar \frac{\partial \psi_1}{\partial t} = -\frac{\hbar^2}{2m_1} \nabla^2 \psi_1 + (V_1 - \mu_1)\psi_1 + U_{11}|\psi_1|^2\psi_1 + U_{12}|\psi_2|^2\psi_1, \quad (1.18)$$

$$i\hbar \frac{\partial \psi_2}{\partial t} = -\frac{\hbar^2}{2m_2} \nabla^2 \psi_2 + (V_2 - \mu_2)\psi_2 + U_{22}|\psi_2|^2\psi_2 + U_{12}|\psi_1|^2\psi_2. \quad (1.19)$$

11

1.3.1 Linearized Excitations

If we linearise the equations for the two components by replacing ψ_k with $\psi_k + \delta\psi_k$, the following are obtained:

$$i\hbar\frac{\delta\psi_1}{\partial t} = -\frac{\hbar^2}{2m_1}\nabla^2\delta\psi_1 + (V_1 - \mu_1)\delta\psi_1 + U_1(2|\psi_1|^2\delta\psi_1 + |\psi_1|^2\delta\psi_1)$$

$$+ U_{12}(|\psi_2|^2\delta\psi_1 + \psi_2^*\psi_1\delta\psi_2 + \psi_1\psi_2\delta\psi_2^*), \quad (1.20)$$

$$i\hbar\frac{\delta\psi_2}{\partial t} = -\frac{\hbar^2}{2m_2}\nabla^2\delta\psi_2 + (V_2 - \mu_2)\delta\psi_2 + U_2(2|\psi_2|^2\delta\psi_2 + |\psi_2|^2\delta\psi_2)$$

$$+ U_{12}(|\psi_1|^2\delta\psi_2 + \psi_1^*\psi_2\delta\psi_1 + \psi_1\psi_2\delta\psi_1^*). \quad (1.21)$$

Therefore, the Bogoliubov equations can be obtained by substituting $\delta\psi_1 = u_{1k}(r)e^{i(kr-\omega t)} - v_{1_k}^*(r)e^{-i(kr-\omega t)}$ and $\delta\psi_2 = u_{2k}(r)e^{i(kr-\omega t)} - v_{2_k}^*(r)e^{-i(kr-\omega t)}$, resulting in four linearised equations in terms of the Bogoliubov parameters:

$$v_{2k}\left[\hbar\omega + \frac{\hbar^2 k^2}{2m_2} + V_2 - \mu_2 + 2U_2 n_2 + U_{12}n_1\right]$$

$$- u_{2k}[U_2 n_2] + v_{1k}[U_{12}\sqrt{n_1 n_2}] - u_{1k}[U_{12}\sqrt{n_1 n_2}] = 0, \quad (1.22)$$

$$v_{1k}\left[\hbar\omega + \frac{\hbar^2 k^2}{2m_1} + V_1 - \mu_1 + 2U_1 n_1 + U_{12}n_2\right]$$

$$- u_{1k}[U_1 n_1] + v_{2k}[U_{12}\sqrt{n_1 n_2}] - u_{2k}[U_{12}\sqrt{n_1 n_2}] = 0, \quad (1.23)$$

$$u_{2k}\left[\hbar\omega - \frac{\hbar^2 k^2}{2m_2} - V_2 - \mu_2 - 2U_2 n_2 - U_{12} n_1\right]$$

$$+ v_{2k}[U_2 n_2] - u_{1k}[U_{12}\sqrt{n_1 n_2}] + v_{1k}[U_{12}\sqrt{n_1 n_2}] = 0, \quad (1.24)$$

$$u_{1k}\left[\hbar\omega - \frac{\hbar^2 k^2}{2m_1} - V_1 - \mu_1 - 2U_1 n_1 - U_{12} n_2\right]$$

$$+ v_{1k}[U_1 n_1] - u_{2k}[U_{12}\sqrt{n_1 n_2}] + v_{2k}[U_{12}\sqrt{n_1 n_2}] = 0. \quad (1.25)$$

The solution obtained for the energy spectrum hence is,

$$\hbar^2\omega^2 = \frac{1}{2}\left[(\alpha_1^2 - U_1^2 n_1^2) + (\alpha_2^2 - U_2^2 n_2^2)\right]$$

$$\pm \frac{1}{2}\left[\sqrt{(\alpha_1^2 - U_1^2 n_1^2) - (\alpha_2^2 - U_2^2 n_2^2) + 16(\alpha_1 - U_1 n_1)(\alpha_2 - U_2 n_2)c}\right], \quad (1.26)$$

where

$$\alpha_1 = \hbar\omega + \frac{\hbar^2 k^2}{2m_1} + V_1 - \mu_1 + 2U_1 n_1 + U_{12} n_2, \quad (1.27)$$

$$\alpha_2 = \hbar\omega + \frac{\hbar^2 k^2}{2m_2} + V_2 - \mu_2 + 2U_2 n_2 + U_{12} n_1, \quad (1.28)$$

$$c = g_{12}\sqrt{n_1 n_2}. \quad (1.29)$$

This gives the dispersion relation for a two-component BEC [Fig. 1.2]. According to the Bogoliubov dispersion relation, oscillations having wavelengths much smaller than the size of the condensate ($\omega \gg \omega_{\text{trap}}$) propagate as free particles. Oscillations with wavelength similar to the length of the condensate are modified from free-particle behaviour. This is consistent with the Bogoliubov theory which predicts that the long wavelength excitations of an interacting Bose gas are sound waves [1, 18].
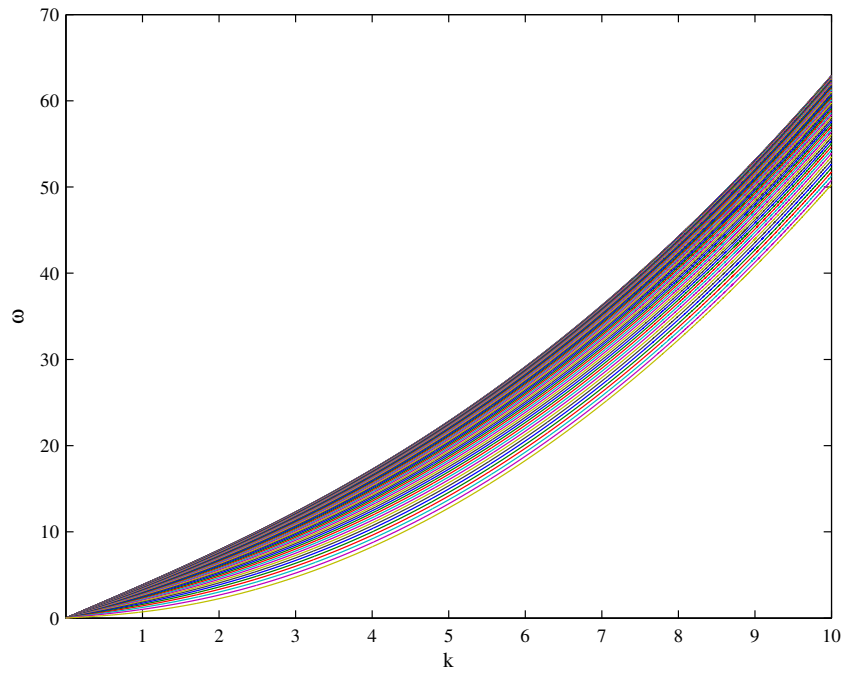
Figure 1.2: Dispersion relation for a two-component BEC showing low and high excitations for the intercomponent interaction strength g_{12} varying from 0 to 1.4, with $g_{11} = 1$ and $g_{22} = 2$.

1.4 Summary

The aim of this chapter was to introduce the GPE in the mean-field regime and to find the dispersion spectrum for one and two-component BECs. It talks about the Bogoliubov approximation, which aids in finding the possible collective excitations and the solution to find the energy spectrum.

Chapter 2

Thomas-Fermi approximation in a circularly symmetric harmonic trap

2.1   Overview

The Thomas-Fermi (TF) approximation is a method to find an approximate analytical solution to the GPE which provide a reasonable description of the system in the miscible region. Since solving the GPE to find the accurate ground state solutions proves to be difficult in terms of gaining understanding of the system, this approximation is a good approach.

This chapter focuses on the applications of the TF approximation to two-component Bose-Einstein condensates in a 2D symmetric harmonic trap in order to find the different regimes that the system has, depending on various parameters. It is in 2D based on the previous successful works done in this area of study which have yielded good results [19, 21].

2.2 Rescaling

By introducing $\eta = \sqrt{N_2/N_1}$, $\zeta = \sqrt{m_2/m_1}$, $\epsilon = \sqrt{\omega_2/\omega_1}$, the GPE can be nondimensionalized by choosing $\hbar = \sqrt{m_1 m_2} = \sqrt{\omega_1 \omega_2} = 1$. On defining the dimensionless intracomponent coupling parameters $g_{kk} = U_k N_k / \hbar^2$ and the intercomponent coupling parameter $g_{12} = U_{12} \sqrt{N_1 N_2}$, the time-independent GPE can be obtained by setting the time derivatives, $\partial \psi_1 / \partial t$, $\partial \psi_2 / \partial t$ as zero. This gives the following coupled equations,

$$\mu_1 \psi_1 = \left(-\frac{\zeta \nabla^2}{2} + V_1(r) + g_{11}|\psi_1|^2 + g_{12}\eta|\psi_2|^2 \right) \psi_1 \tag{2.1}$$

and

$$\mu_2 \psi_2 = \left(-\frac{\nabla^2}{2\zeta} + V_2(r) + g_{22}|\psi_2|^2 + g_{12}\frac{|\psi_1|^2}{\eta} \right) \psi_2, \tag{2.2}$$

where the rescaled trapping potential for each component is

$$V_1(r) = \frac{r^2}{2\zeta \epsilon^2}, \tag{2.3}$$

$$V_2(r) = \frac{\zeta \epsilon^2 r^2}{2}. \tag{2.4}$$

The ground state of the coupled GPE is subject to the normalization condition as

$$\int |\psi_k|^2 \, d^2 r = 1. \tag{2.5}$$

Considering only repulsive interactions, i.e the case where g_1, g_2 and g_{12} are always non-negative, we define a dimensionless parameter combining the g_k and g_{12} in order

to separate the regimes of interest:

$$\Gamma_{12} = 1 - \frac{g_{12}^2}{g_{11}g_{22}}.$$ (2.6)

2.3 Thomas-Fermi solution

For considerably large interaction strengths or particle number, the ground state solution can be obtained by neglecting the kinetic energy term in the GPE [1, 2, 6]. This is known as the Thomas-Fermi approximation. For a BEC in a harmonic trap, it is known that with repulsive interactions between a large number of atoms, the ratio of the kinetic energy to the potential energy is small. Hence we can ignore the kinetic energy term. According to the TF approximation, neglecting $\nabla^2\psi_1$ and $\nabla^2\psi_2$,

$$\mu_1 = \frac{r^2}{2\zeta\epsilon^2} + g_{11}|\psi_1^2| + g_{12}\eta|\psi_2|^2,$$ (2.7)

$$\mu_2 = \frac{\zeta\epsilon^2 r^2}{2} + g_{22}|\psi_2^2| + \frac{g_{12}}{\eta}|\psi_1|^2.$$ (2.8)

Solving these two equations simultaneously, we get the Thomas-Fermi solutions as

$$|\psi_1|^2 = \frac{1}{g_{11}\Gamma_{12}}\left[\mu_1 - \frac{r^2}{2\zeta\epsilon^2} - \frac{g_{12}\eta}{g_{22}}\left(\mu_2 - \frac{\zeta\epsilon^2 r^2}{2}\right)\right]$$ (2.9)

and

$$|\psi_2|^2 = \frac{1}{g_{22}\Gamma_{12}}\left[\mu_2 - \frac{\zeta\epsilon^2 r^2}{2} - \frac{g_{12}}{g_{11}\eta}\left(\mu_1 - \frac{r^2}{2\zeta\epsilon^2}\right)\right],$$ (2.10)

where μ_1 and μ_2 are determined from the normalization condition stated in Eq. (2.5).

2.3.1 Critical Value for the Thomas-Fermi approximation

The TF approximation for two components is a good approximation only within a particular range of the interaction strengths. To elucidate this, we first consider the case where $V_1 = V_2 = 0, \eta = 1$ and the masses for the both the components are equal, the stationary state densities of the two components can be written as:

$$|\psi_1|^2 = \frac{\mu_1 - \frac{g_{12}}{g_{22}}\mu_2}{g_{11}\Gamma_{12}}, \tag{2.11}$$

$$|\psi_2|^2 = \frac{\mu_2 - \frac{g_{12}}{g_{11}}\mu_1}{g_{22}\Gamma_{12}}. \tag{2.12}$$

Upon invoking the TF limit we find the chemical potentials to be

$$\mu_1 = g_{11}n_1 + g_{12}n_2, \mu_2 = g_{22}n_2 + g_{12}n_1, \tag{2.13}$$

where $|\psi_k|^2 = n_k$. Substituting Eq. (2.13) into Eq. (1.25) gives the dispersion relation,

$$\omega = k\sqrt{(1/m) + [(A - \sqrt{A^2 + B}))/m]\frac{1}{2}} \tag{2.14}$$

where $A = g_{11}n_1 + g_{22}n_2, B = 4n_1n_2(g_{12}^2 - g_{11}g_{22})$.

From Eq. (2.14) we can see that the term $A - \sqrt{A^2 + B}$ becomes greater than 0 for $B < 0, A^2 + B < A$, and less than 0 for $B > 0, A^2 + B > A^2$, which implies that the solutions now become imaginary, as $k \to 0$. Since the frequency of the oscillations cannot be imaginary, $B = 0 \leftrightarrow 4n_1n_2(g_{12}^2) - g_{11}g_{22} = 0$, becomes a critical value. If $g_{12}^2 > g_{11}g_{22}$, ω_-^2 becomes negative as the energy levels are repelled strongly due to the intercondensate interaction. This gives the longer wavelengths modes that grow

exponentially, making the homogeneous system unstable [22]. The TF approximation becomes void as one gets closer to the critical value. The contribution of the kinetic energy terms becomes more significant and the condensate approaches the immiscible regime. For a homogeneous system, immiscibility requires the interaction strengths to satisfy $g_{12}^2 > g_{11}g_{22}$ [1, 2, 22, 23]. The critical value for the interaction strength is hence,

$$g_{\text{crit}} = \sqrt{g_{11}g_{22}}.$$
(2.15)

2.4 Different cases in a 2D two-component condensate in a harmonic trap

For $g_{11} < g_{22}$ it has been observed that the value of the interaction term between the two components (g_{12}) affects the behaviour of the condensate in terms of the different phases of the condensate. The limits for the two densities are decided by predetermining the shape of the condensates. The BEC system can be categorized based on the number of regions in the system. The first is having two disks. In a two-component BEC system with a symmetric harmonic trap one can observe two regions: First, the region where both the components coexist; second, the region where only one of the condensates exists. The second case where there are three regions which can be described as: First, the region where only the first component exists; second, where both the components coexist; and third, where only the second component exists [19, 21].

2.4.1 Case I: Both components are disks

In order to find the different radii and the chemical potentials, we start when both components are disks [Fig. 2.1]. Assume that the outer boundary of the component 2 (at $r = R_2$) is larger than that of the component 1 (at $r = R_1$). We can find the two radii (R_1 and R_2) for the case where two disks are formed and the two chemical potentials for this case (μ_1 and μ_2) by simultaneously solving these equations for the densities of the two components and the condition for their normalization, to find the four unknowns. This gives the following solutions,

$$\mu_1 = \left(\frac{\bar{g}_{11}\Gamma_{12}\Gamma_2}{\pi}\right)^{\frac{1}{2}} + \frac{g_{12}}{g_2}\eta\mu_2, \tag{2.16}$$

$$\mu_2 = \left(\frac{\lambda^2(\bar{g}_{22} + \bar{g}_{12}/\eta)}{\pi}\right)^{\frac{1}{2}}, \tag{2.17}$$

$$R_1 = \left(\frac{4\bar{g}_{11}\Gamma_{12}}{\pi\Gamma_2}\right)^{\frac{1}{4}}, \tag{2.18}$$

$$R_2 = \left(\frac{4[\bar{g}_{22} + \bar{g}_{12}\eta]}{\pi\lambda}\right)^{\frac{1}{4}}, \tag{2.19}$$

where $\lambda = \zeta\epsilon^2$ and $\Gamma_2 = 1/\lambda\left(1 - \lambda^2 g_{12}\eta/g_{22}\right)$. When both components are present, the densities of the two components are given in terms of Eq. (2.9) and Eq. (2.10). When only one component is present ($\psi_1\psi_2 = 0$), this simplifies to

$$n(r) = \begin{cases} \left(\mu_2 - \frac{\zeta\epsilon^2 r^2}{2}\right)\frac{1}{g_{22}}, & \text{if } \psi_1 = 0, \\ \left(\mu_1 - \frac{r^2}{2\zeta\epsilon^2}\right)\frac{1}{g_{11}}, & \text{if } \psi_2 = 0. \end{cases}$$

Figure 2.1: Thomas-Fermi solutions for different cases when both the components are disk shaped, showing two regions: a region with both the components and a region where only one component is present. r_{HO} is the radius of the harmonic oscillator. In all cases, $g_1 = 3000$, $g_2 = 5000$, $\zeta = 1$, $\epsilon = 1$, $\eta = 1$. Plots (a) and (b) are cases with g_{12} as 0 and 1000, respectively.
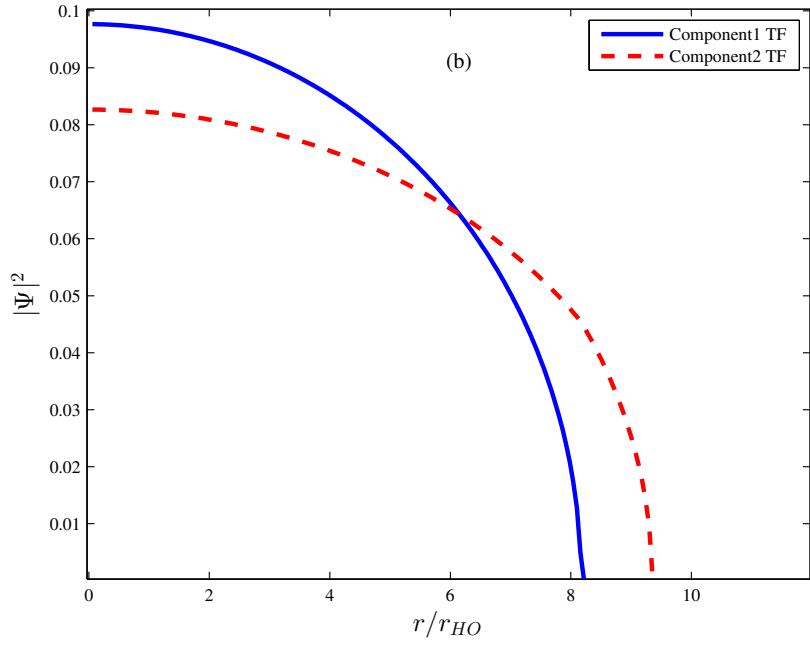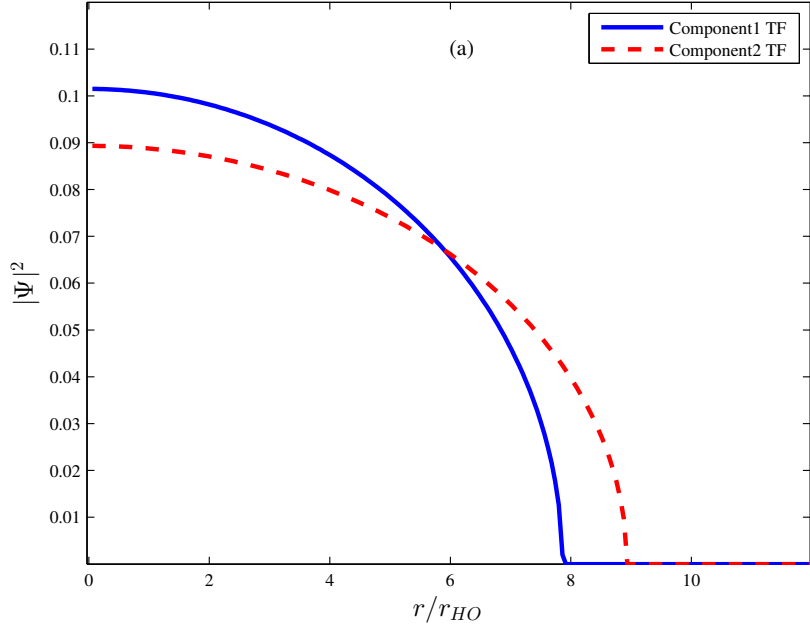
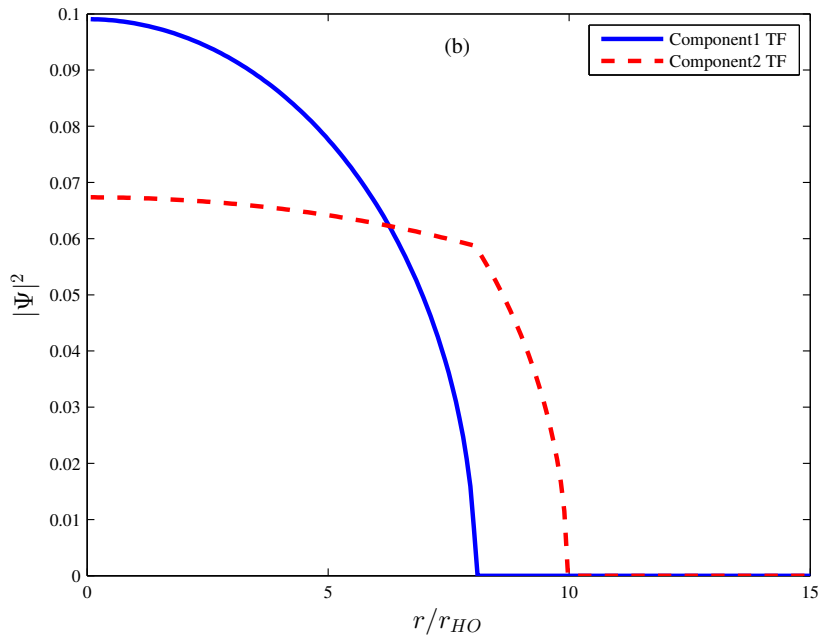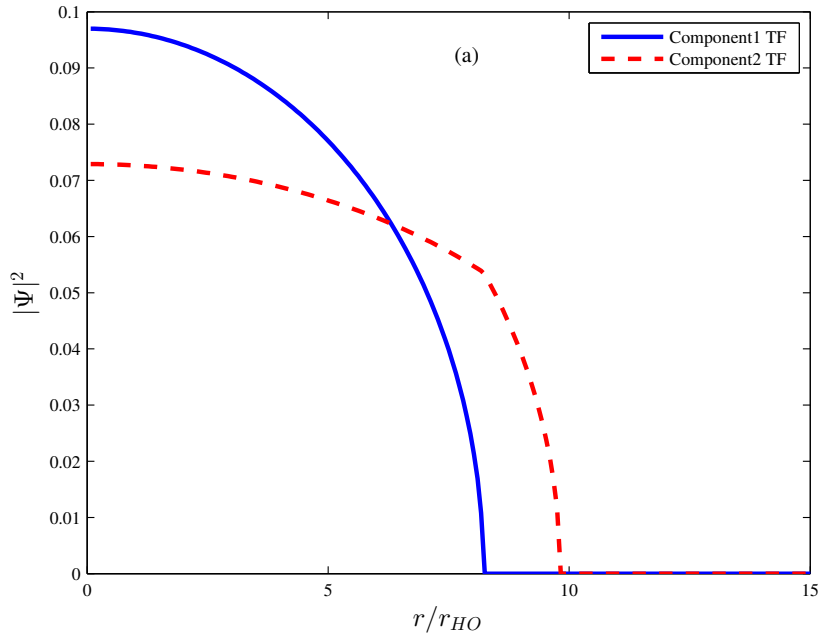Figure 2.2: Thomas-Fermi solutions for different cases when both the components are disk shaped, showing two regions: a region with both the components and a region where only one component is present. r_{HO} is the radius of the harmonic oscillator. In all cases, $g_1 = 3000$, $g_2 = 5000$, $\zeta = 1$, $\epsilon = 1$, $\eta = 1$. Plots (a) and (b) are cases with g_{12} as 2300 and 2750, respectively.

When g_{12} equals the value of g_{11}, the density profile one gets for the second component is a straight line for $r < R_1$. This is the value after which the two disks case starts transitioning into a disk plus a disk with a dip and eventually transitioning into the disk plus annulus case [Fig. 2.2].

Having the boundary condition that $|\psi_2|^2 = 0$ at $r = 0$, and using Eq. (2.15), one can write

$$g_{12} = \frac{g_{11}\eta\mu_2}{\left(\frac{g_{11}\Gamma_{12}\Gamma_2}{\pi}\right)^{1/2} + \frac{g_{12}}{g_{22}}\eta\mu_2}. \tag{2.20}$$

This takes places when the value of the interaction between the two condensates (g_{12}) for when the condensate transitions into an annulus is equal to g_{12}^{ann} [Fig. 2.3(a)]. This value is found to be,

$$g_{12}^{\text{ann}} = \frac{g_{11}\eta}{2(1 + \eta)} \pm \frac{1}{2}\sqrt{\frac{g_{11}^2\eta^2}{(1 + \eta)^2} + \frac{4\eta g_{11}g_{22}}{1 + \eta}}. \tag{2.21}$$

2.4.2   Case II: A disk and an annular component

Assuming that component 1 is a disk and component 2 is an annulus, the condensate can be separated into three regions: an inner disk where only component 1 is present, an outer annulus where only component 2 is present, and an inner annulus where both components coexist [Fig. 2.4]. The inner disk's boundary is marked by R_1, and R_2^- and R_2^+, defining the inner and outer boundary layer of the annulus and μ_1 and μ_2 are the

Figure 2.3: Thomas-Fermi solutions for different cases from when both the components are disk shaped, transitioning to the disk plus annulus case, showing two regions: a region with both the components and a region where only one component is present. r_{HO} is the radius of the harmonic oscillator. In all cases, $g_1 = 3000$, $g_2 = 5000$, $\zeta = 1$, $\epsilon = 1$, $\eta = 1$. For plots (a) and (b), the cases are with g_{12} as 3000 and 3560, respectively.

chemical potentials for the two components, given as

$$R_2^{+2} = \frac{2}{\lambda}\left[\sqrt{\frac{\lambda g_1(\eta + 1)}{\pi}} + \sqrt{\frac{g_1 g_2 \Gamma_1 \Gamma_{12}}{\pi g_{12}}}\right], \quad (2.22)$$

$$R_2^{-2} = \frac{2}{\lambda}\left[\sqrt{\frac{\lambda g_1(\eta + 1)}{\pi}} - \sqrt{\frac{-g_1 g_2 \Gamma_2}{\pi g_{12}\Gamma_1}}\right], \quad (2.23)$$

$$R_1^2 = \frac{2}{\lambda}\left[\sqrt{\frac{\lambda g_1(\eta + 1)}{\pi}} - \sqrt{\frac{-g_1 g_{12}\Gamma_1}{\pi g_2 \Gamma_2}}\right], \quad (2.24)$$

$$\mu_1 = \frac{\lambda g_1}{\pi}(\eta + 1) \quad (2.25)$$

$$\mu_2 = \mu_1 + \sqrt{\frac{-g_1 g_2 \Gamma_1 \Gamma_{12}}{\pi g_{12}}}. \quad (2.26)$$

2.5   Limitations

As one gets closer to the critical value for g_{12}, i.e when $g_{12}^2 > g_1 g_2$ (section 2.3), the condensate mixture approaches towards the immiscible region from the miscible region. It is seen that the Thomas-Fermi approximation starts to fail and is not as good an estimation beyond this value. The TF approximation is a good tool only within the miscible regime and when the interaction strength (g_{12}) is lower than the critical interaction value. This is so because as the system gets closer to phase separation, the value of the kinetic energy term is no longer small when compared to the other energies and hence needs to be accounted for while calculating the ground state solutions. As one approaches the critical value for the interaction strengths, the TF solutions appear to be more sharp [Fig. 2.5].
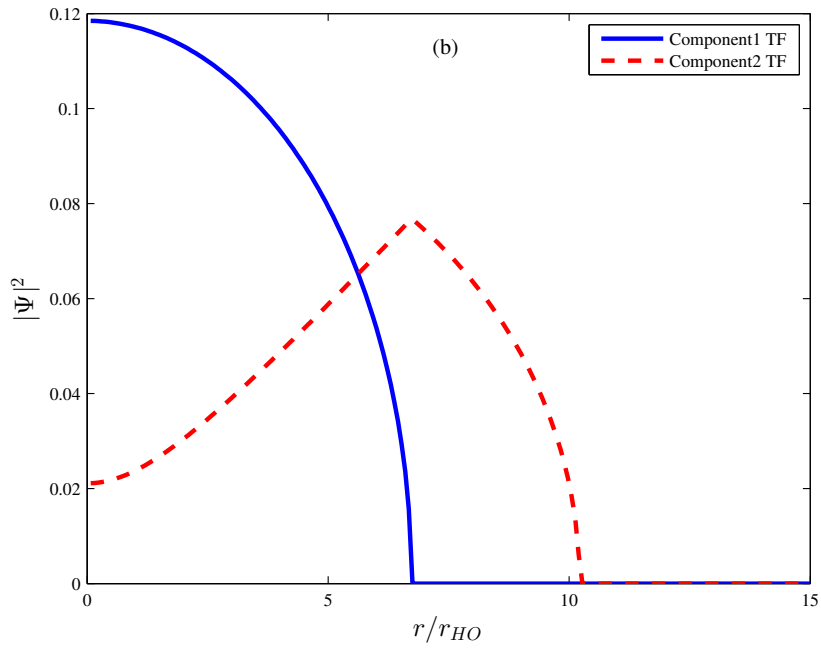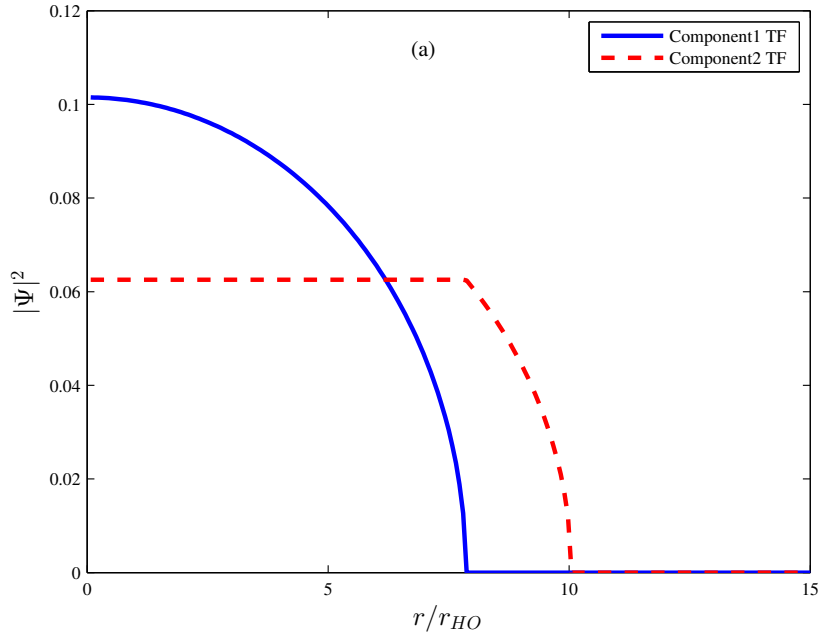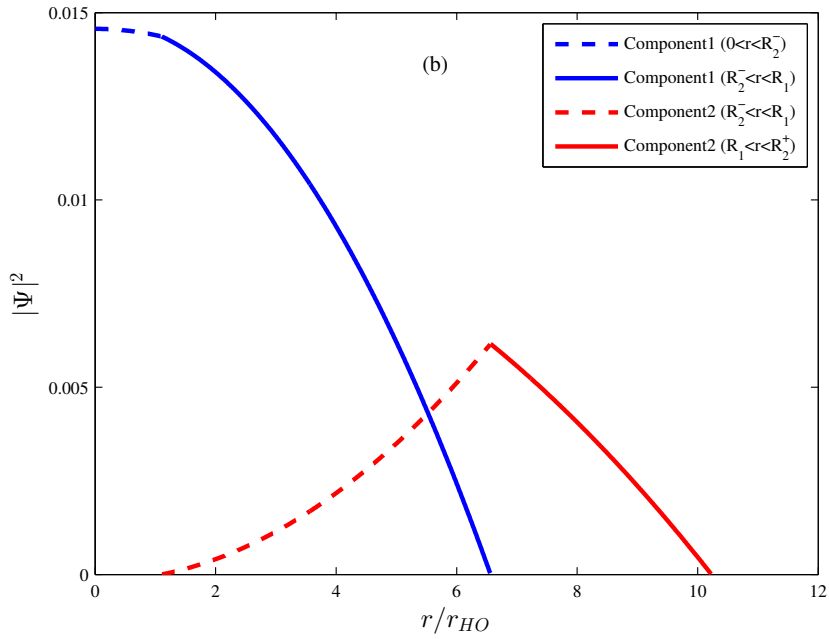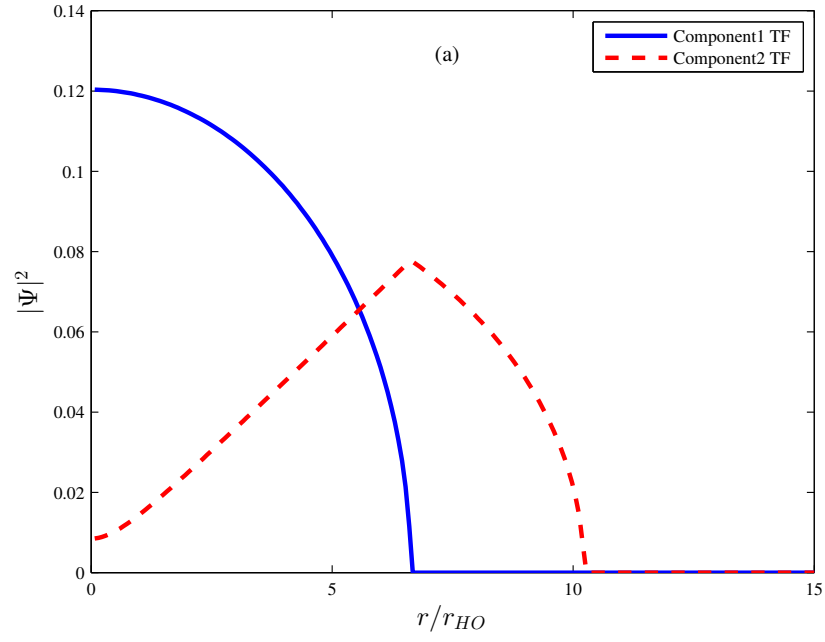
Figure 2.4: Thomas-Fermi solutions for different cases from when both the components are disk shaped, transitioning to the disk plus annulus case. r_{HO} is the radius of the harmonic oscillator. In all cases, $N_1 = N_2 = 1 = \eta$, $g_1 = 3000$, $g_2 = 5000$, $\zeta = 1$, $\epsilon = 1$. Plots (a) and (b) are cases with g_{12} as $3585 (\simeq g_{12}^{\mathrm{ann}})$, 3600.

2.6 Summary

The TF approximation is useful way of studying a two-component BEC and allows us to classify its ground states in terms of whether the condensate components coexist or are spatially separated. However, this approximation is applicable only within the critical value (g_{crit}) [Eq. (2.15)] beyond which the assumptions made are void. Therefore, it is essential to come up with a more reliable method in order to obtain a better understanding of the condensate mixture, without having to solve the GPE by itself. From the TF solutions and looking at the different cases obtained, one can infer that
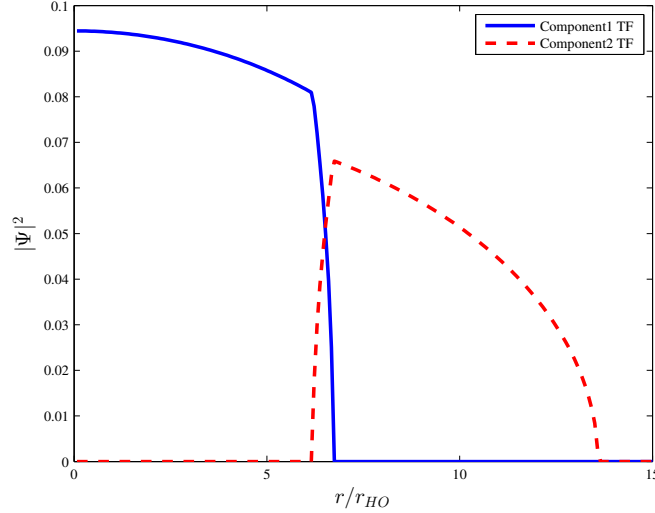
Figure 2.5: Plot showing the TF solution for the case where the interaction strength (g_{12}), is very close to the critical limit, for $N_1 = N_2 = 1 = \eta$, $g_1 = 3000$, $g_2 = 5000$, $\zeta = 1$, $\epsilon = 1$. The values of $g_{11}, g_{22},$ and g_{12} are 8000, 16000 and $\sqrt{0.98g_{11}g_{22}}$, respectively.

if $g_{22} \gg g_{11}$, Γ_{12} evaluated at $g_{12} = g_{11}g_{22}$ tends to unity. An annulus in this case will be present in component 2, whatever may be the value of g_{12} [19]. When given that the particle number ($N = N_1 = N_2$) for both the components is the same, $\eta = 1$. This means that the TF solution is independent of N_k. And the case where the particle number is not the same for both component, the solution varies only by a ratio, η.

Chapter 3

GPE ground state solutions

3.1 Overview

This chapter talks about how to numerically calculate the ground state solutions for the GPE by numerically solving it and comparing the results obtained with the TF solutions. The programme basically calculates the complete numerical solutions using the finite difference method, further using the discretized GPE written in the form of matrices and then finding the Jacobian matrix for those and solving the complete set of nonlinear second order differential equations. The process can be divided into three main sections: first, the section which defines the GPE for a given dimension; second, the section to calculate the time stepping using a finite difference scheme; and third, the section wherein the nonlinear equations are solved.

3.2 General equation and different dimensionalities

The two-component GPE for the case with same particle number, same masses and same trapping frequency for both the components can be written as,

$$\left[-\frac{\nabla^2}{2} + V(r) + g_{k,k}|\psi_k|^2 + g_{k,3-k}|\psi_{3-k}|^2 - \mu_k\right]\psi_k = 0, \tag{3.1}$$

for k=1,2, and where the normalization condition is set to be

$$\int |\psi_k(r)|^2 dr = 1. \tag{3.2}$$

The Laplacian can be written in each dimension for a spherically symmetric case. In 3D with spherical symmetry, one has

$$\begin{aligned}
\nabla^2 &= \frac{1}{r^2}\frac{\partial}{\partial r}\left(r^2\frac{\partial}{\partial r}\right) \\
&= \frac{2}{r}\frac{\partial}{\partial r} + \frac{\partial^2}{\partial r^2}.
\end{aligned} \tag{3.3}$$

In 2D with circular symmetry, one has

$$\begin{aligned}
\nabla^2 &= \frac{1}{r}\frac{\partial}{\partial r}\left(r\frac{\partial}{\partial r}\right) \\
&= \frac{1}{r}\frac{\partial}{\partial r} + \frac{\partial^2}{\partial r^2}.
\end{aligned} \tag{3.4}$$

And in 1D with reflection symmetry about the origin, one has

$$\nabla^2 = \frac{\partial^2}{\partial r^2}. \tag{3.5}$$

The GPE code [24] focuses on the 2D case with circular symmetry and so for the purpose of this study only Eq. (3.4) will be utilized. The normalization condition in 2D is therefore taken to be

$$\int 2\pi r |\psi_k(r)|^2 dr = 1.$$

(3.6)

3.3 Finite difference scheme

The first step is to define the boundary conditions for the system. The Neumann boundary condition gives the value of the derivative of a solution that it has to take at the boundary of the system [25]. For all dimensions, one can define the Neumann boundary condition at the origin as

$$\left.\frac{\partial \psi_k}{\partial r}\right|_{r=0} = 0.$$

(3.7)

and for a numerical solution on a grid $0 \le r < R_0$, one then uses the Dirichlet condition

$$\psi_k(R_0) = 0$$

(3.8)

which gives the values for the solution to take along the boundary.

Further on, one then uses a central finite difference approximation on a grid of N points such that, $r_j = j * \Delta r$ for $\Delta r = R/N$ and $j \in 1....N$. The normal central difference approximation for the second derivative, on such a grid, is given as

$$\begin{aligned} \partial^2 \psi_{k,i} &= \left.\frac{\partial^2 \psi_{k,i}}{\partial^2 r}\right|_{r=r_i} \\ &= \frac{\psi_{k,i+1} - 2\psi_{k,i} + \psi_{k,i-1}}{\Delta r^2}, \end{aligned}$$

(3.9)

and for the first derivative as

$$\partial \psi_{k,i} = \left. \frac{\partial \psi_{k,i}}{\partial r} \right|_{r=r_i}$$

$$= \frac{\psi_{k,i+1} - \psi_{k,i-1}}{2\Delta r}. \tag{3.10}$$

For the above defined standard finite-difference expressions the implicit Dirichlet boundary conditions are

$$\psi_k(r = R + \Delta r) \;\; = \;\; 0, \tag{3.11}$$

$$\psi_k(r = 0) \;\; = \;\; 0. \tag{3.12}$$

For the system that is being studied here, the first of these is suitable (i.e. having $R_0 = R + \Delta r$). The second must be replaced by the boundary condition at the origin. The second order *forward difference* approximation for the derivative at the origin is

$$\frac{\partial \psi_k}{\partial r} = \frac{-\psi_{k,2} + 4\psi_{k,1} - 3\psi_k(r = 0)}{2\Delta r}, \tag{3.13}$$

and hence to ensure that the derivative is zero at the origin one should take

$$\psi_k(r = 0) = \frac{4\psi_{k,1} - \psi_{k,2}}{3}. \tag{3.14}$$

Back-substituting Eq. (3.14) into the central difference formulae Eq. (3.11) and Eq. (3.12) for $i = 1$ yields

$$\partial^2 \psi_{k,1} \;\; = \;\; \frac{2(\psi_{k,2} - \psi_{k,1})}{3\Delta r^2}, \tag{3.15}$$

$$\partial \psi_{k,1} \;\; = \;\; \frac{2(\psi_{k,2} - \psi_{k,1})}{3\Delta r}. \tag{3.16}$$

31

Thus replacing Eq. (3.09) and Eq. (3.10) with Eq. (3.15) and Eq. (3.16) yields a correct second-order finite-difference representation of the derivative operators on the grid.

3.4 Nonlinear equation solver

Upon defining the boundary conditions, one can then define the derivative matrices, D_{ij} and $D_{ij}^{(2)}$, from the above section using Einstein convention of summation, such that

$$\partial^2 \psi_{k,i} = D_{ij}^{(2)} \psi_{k,j}, \tag{3.17}$$

$$\partial \psi_{k,i} = D_{ij} \psi_{k,j}. \tag{3.18}$$

One can write Eq. (3.1) in terms of Eq. (3.18) and Eq. (3.19) as the discrete equation

$$\left[-\frac{D_{ij}^{(2)}}{2} - \frac{\alpha_{im}}{2} D_{mj} + \delta_k \left(V(r_i) + g_{k,k}|\psi_{k,i}|^2 + g_{k,3-k}|\psi_{3k,i}|^2 - \mu_k \right) \right] \psi_{k,j} = 0, \tag{3.19}$$

where α_{im} is a diagonal matrix dependent on the dimension, and the chemical potential μ_k should be explicitly calculated via

$$\mu_k = \psi_{k,n} \beta_{k,ni} \left[-\frac{D_{ij}^{(2)}}{2} - \frac{\alpha_{im}}{2} D_{mj} + \delta_k \left(V(r_i) + g_{k,k}|\psi_{k,i}|^2 + g_{k,3-k}|\psi_{3k,i}|^2 \right) \right] \psi_{k,j}, \tag{3.20}$$

where δ_k is the Kronecker delta ($\delta_k(x = 0) = 1, \delta_k(x \neq 0) = 0$). The diagonal matrices α and β in 2D are given by

$$\alpha_{ij} = 0 \tag{3.21}$$

32

and

$$\beta_{k,ij} = 2\pi r_i \delta_{ij} \Delta r. \tag{3.22}$$

Upon substituting Eq. (3.20) into Eq. (3.19), one has a nonlinear system of $2N$ equations in $2N$ real variables;

$$G_{k,i}(\psi_{l,j}) = 0, \tag{3.23}$$

for $k, l = 1, 2$, and $i, j = 1...N$. Defining the Jacobian matrix

$$J_{kl,ij} = \frac{\partial G_{k,i}}{\partial \psi_{l,j}}, \tag{3.24}$$

such that,

$$J = \begin{bmatrix} \frac{\partial G_i^{(1)}}{\partial \psi_j^{(1)}} & \frac{\partial G_i^{(1)}}{\partial \psi_j^{(2)}} \\ \frac{\partial G_i^{(2)}}{\partial \psi_j^{(1)}} & \frac{\partial G_i^{(2)}}{\partial \psi_j^{(2)}} \end{bmatrix}. \tag{3.25}$$

The Jacobian is explicitly given by

$$J_{11,ij} = \left[-\psi_1 \left(\frac{\partial \mu_1}{\partial \psi_j} \right)^{\mathrm{T}} \right] - \frac{D_{ij}}{2} - \frac{\alpha_{im}}{2} D_{mj} + \delta_{ij}(V_j - \mu_1 + (3g_{11}|\psi_i|^2 + g_{12}|\psi_j|^2)), \tag{3.26}$$

$$J_{22,ij} = \left[-\psi_2 \left(\frac{\partial \mu_2}{\partial \psi_j} \right)^{\mathrm{T}} \right] - \frac{D_{ij}}{2} - \frac{\alpha_{im}}{2} D_{mj} + \delta_{ij}(V_j - \mu_2 + (3g_{22}|\psi_j|^2 + g_{12}|\psi_i|^2)), \tag{3.27}$$

$$J_{12,ij} = \delta_{ij}(2g_{12}\psi_i\psi_j) - (\psi_1 2\Delta r(g_{12}|\psi_i|^2\psi_j r)^{\mathrm{T}})2\pi, \tag{3.28}$$

$$J_{21,ij} = \delta(2g_{12}\psi_{ii}\psi_{jj}) - (\psi_2 2\Delta r(g_{12}|\psi_j|^2\psi_i r)^{\mathrm{T}})2\pi, \tag{3.29}$$

one can find the numerical solution efficiently using the built-in Matlab `fsolve` routine [25], given the TF profile as a suitably close initial guess [24].

33

Figure 3.1: Numerical ground state solutions to the GPE along with the TF solution. Plots (a) and (b) show the solutions for the case where both components are disks, with $g_{11} = 3000$ and $g_{22} = 5000$ and their values of g_{12} as 0 and 1000, respectively. r_{HO} is the radius of the harmonic oscillator.

Figure 3.2: Numerical ground state solutions to the GPE along with the TF solution. Plots (a) and (b) show the solutions for the case where both components are disks, with $g_{11} = 3000$ and $g_{22} = 5000$ and their values of g_{12} as 2300 and 2750, respectively. r_{HO} is the radius of the harmonic oscillator.
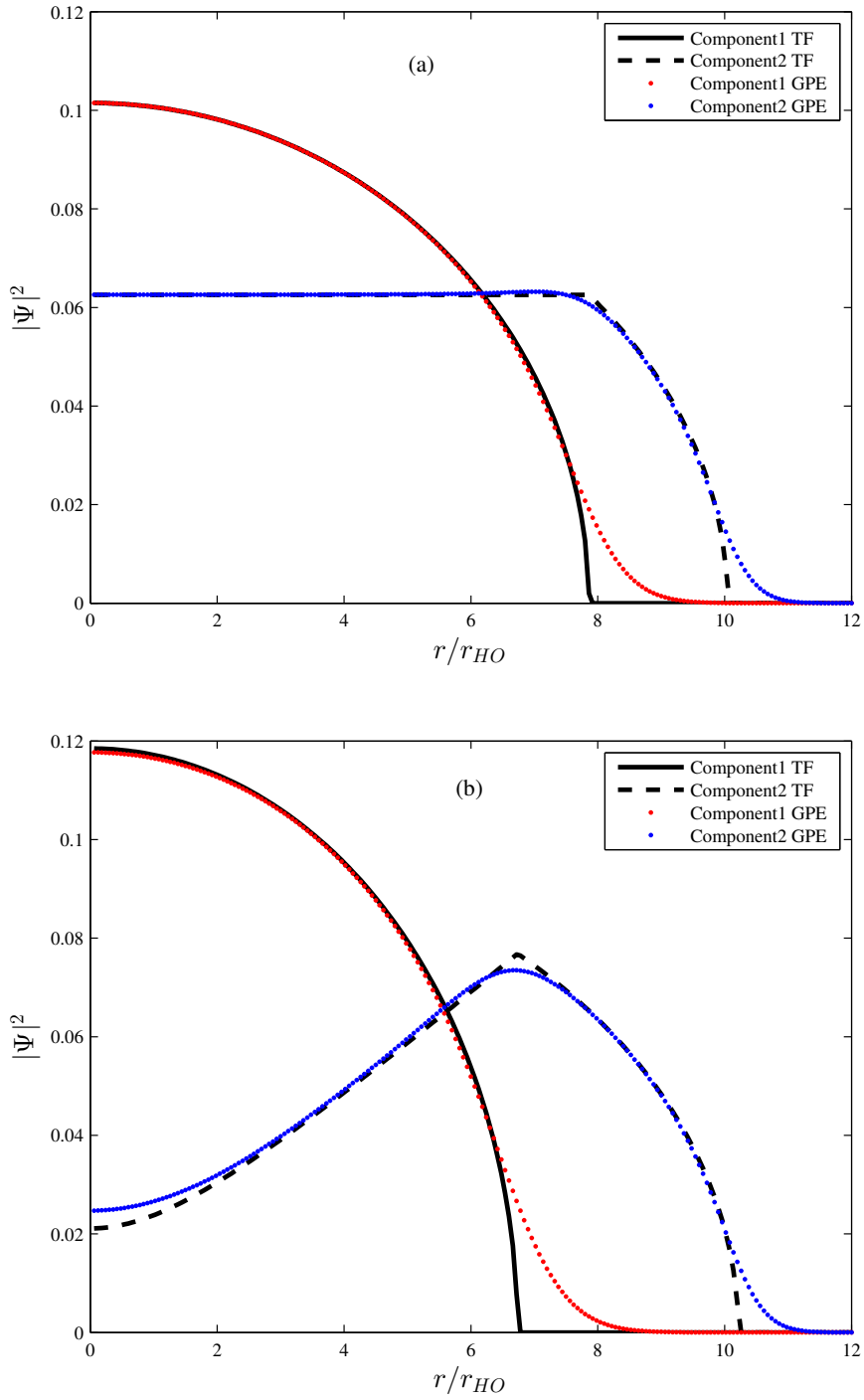
Figure 3.3: Numerical ground state solutions to the GPE along with the TF solution. Plots (a) and (b) show the solutions for the case where both components are disks, with $g_{11} = 3000$ and $g_{22} = 5000$ and their values of g_{12} as 3000 and 3560, respectively. r_{HO} is the radius of the harmonic oscillator.
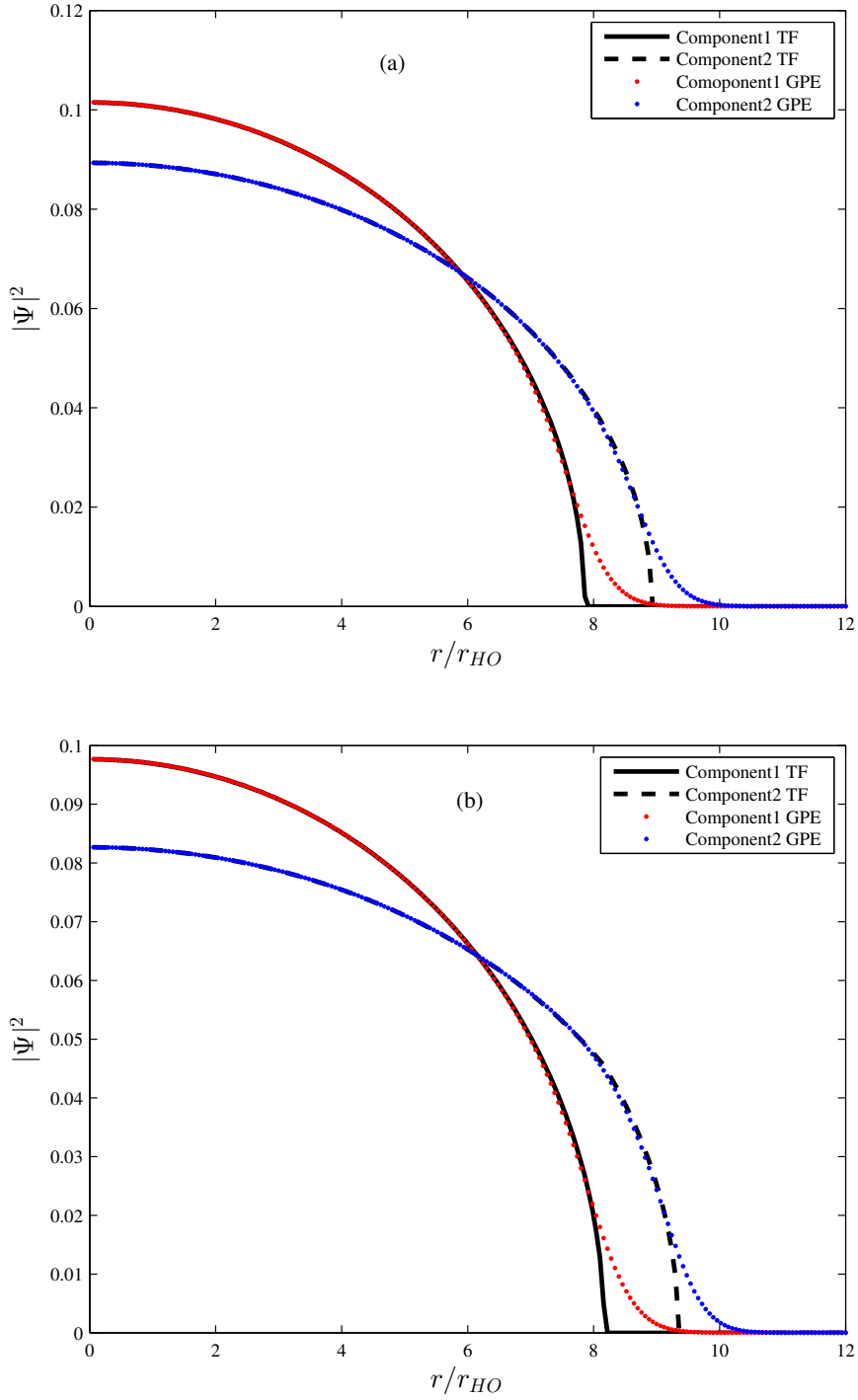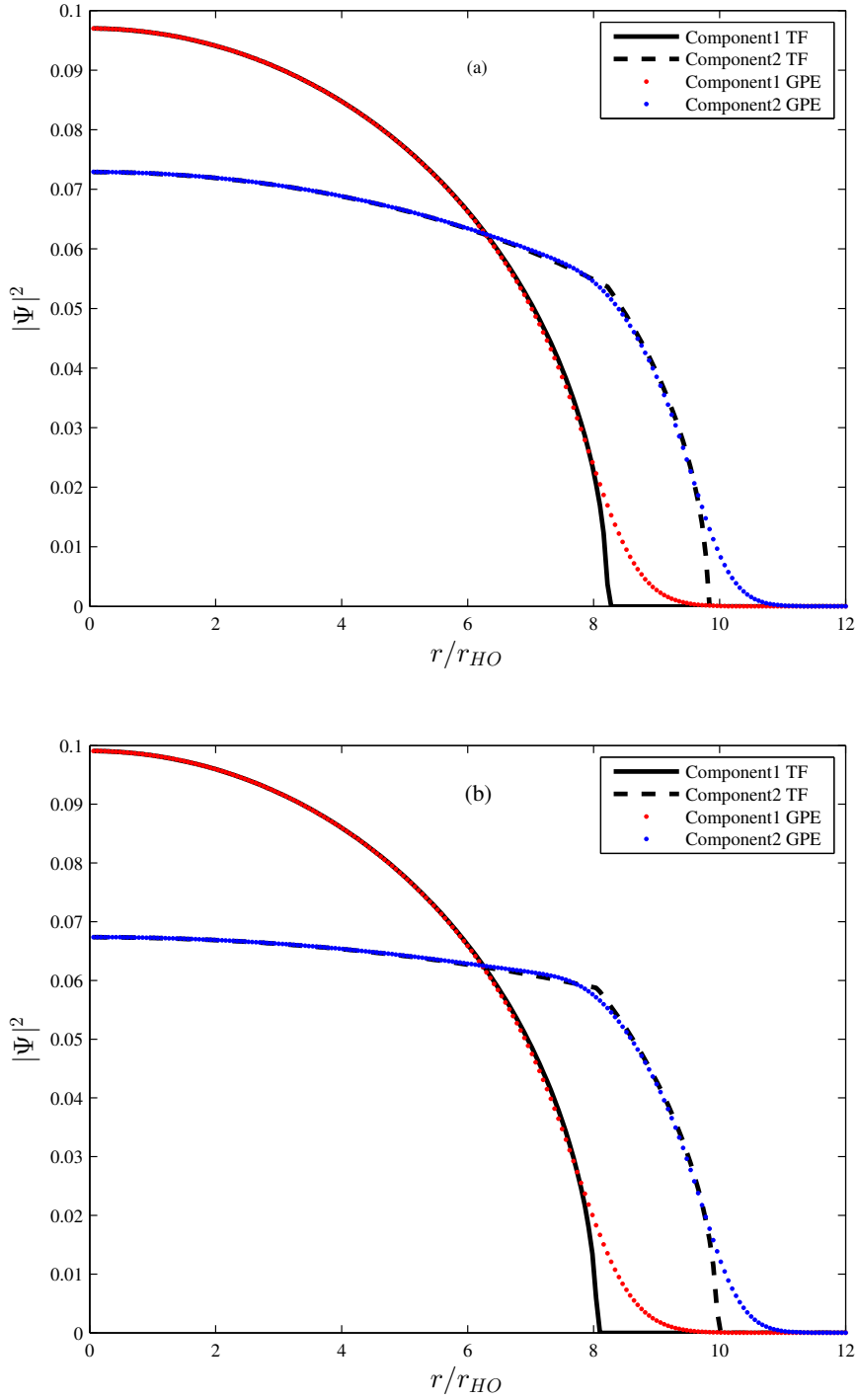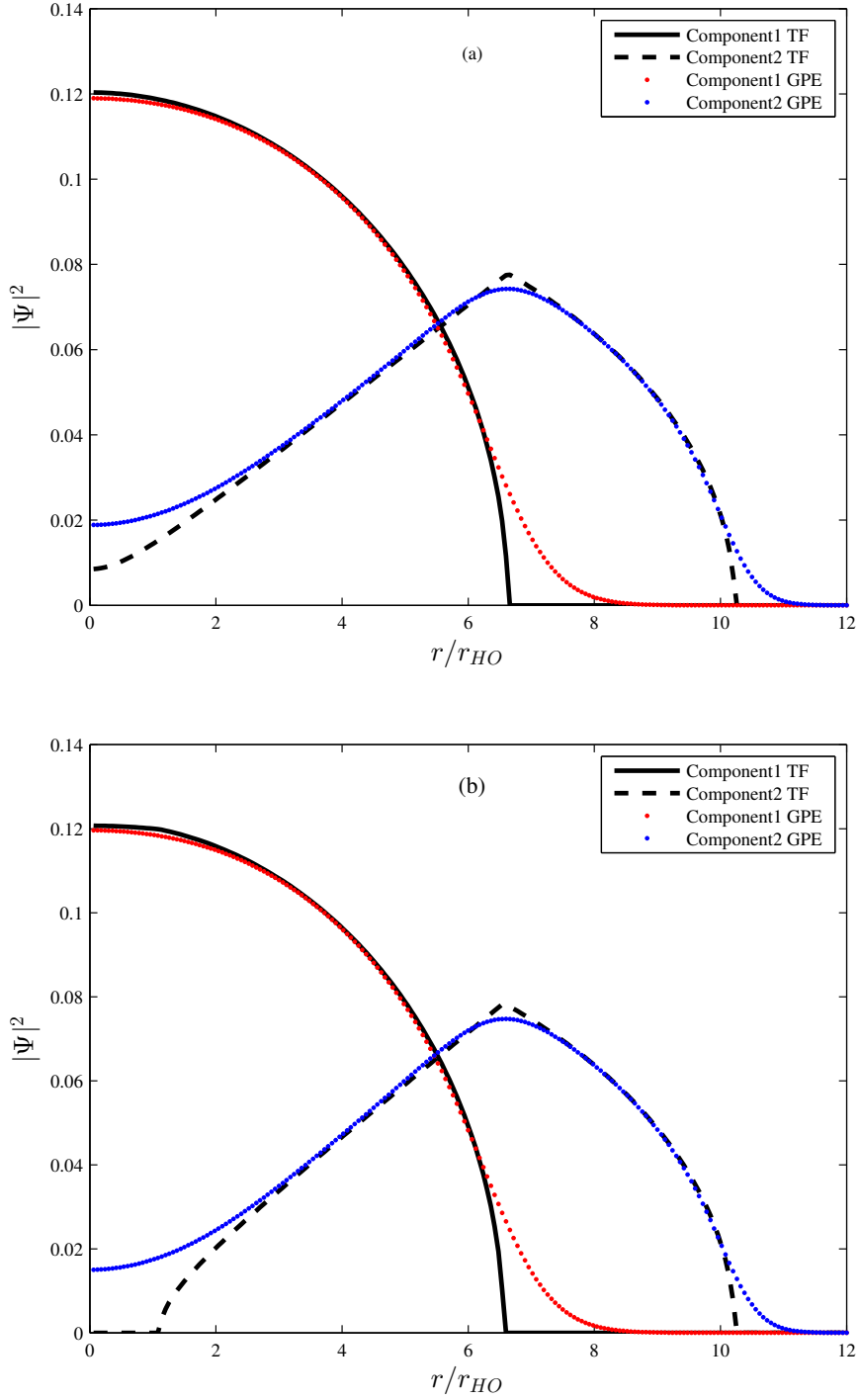
Figure 3.4: Numerical ground state solutions to the GPE along with the TF solution. Plots (a) and (b) show the solutions for the case where both components are disks, with $g_{11} = 3000$ and $g_{22} = 5000$ and their values of g_{12} as $3585 (\simeq g_{12}^{\text{ann}})$ and 3600, respectively. r_{HO} is the radius of the harmonic oscillator.

3.5   Summary

The ground state solutions to the GPE can be found by numerically solving the two coupled equations using the Thomas-Fermi solutions as a reference solution. If one compares the TF solutions with the exact numerics, it can be seen that the TF solutions start to fail as they get closer to the values of the critical radii. The TF approximation gives sharper solutions. However, the numerics of the GPE suggest otherwise. The GPE solutions are continuous and smooth even as one tends towards the TF limit.

Chapter 4

Beyond the Thomas-Fermi limit

4.1 Overview

When the gas cloud becomes very low in density, near the boundaries where the densities tend to zero, the contribution of the kinetic energy becomes more significant and is no longer negligible. The Thomas-Fermi (TF) approximation starts to fail at this point. In order to investigate the behaviour of the condensate wave function at the boundary of the trapped gas, we adapt the method used in [26, 27] for a single-component condensate to a two-component condensate. This chapter discusses in detail a method to approximate the wave function around the regions where TF fails and one can no longer neglect the contribution of kinetic energy.

4.2 Cases

The two-component system can be explained by separating it into three different regions. One region is the outermost part where there is only one component present; the

other two regions are where there is with only one component on one side of a critical radius and both components coexisting on the other side. The following subsections provide a detailed understanding of the method adapted to give a better approximation near these boundary layers, for a two-condensate mixture with the equal numbers of particles.

4.2.1 Two disks

We first consider the case with equal masses ($m_1 = m_2$), equal numbers of particles ($N_1 = N_2$) and equal trapping frequencies ($\omega_1 = \omega_2$). Near the outer boundary of the system, only component 2 is present [Fig. 4.1]. For values of r much larger than the thickness of the boundary, the second term $\left(\frac{1}{r}\nabla\psi_2\right)$ of Eq. (3.4) is negligible. Let R_2 be the outermost boundary of the system, determined by the equation $\mu_2 = V_{\text{ext}_2}(R_2)$. Close to this point, when $|r - R_2| \ll R_2$, one can carry out the following expansion,

$$V_{\text{ext}_2}(r) - \mu_2 = (r - R_2)F + o(r - R_2), \tag{4.1}$$

where F is the modulus of the attractive external force $\vec{F} = -\nabla V_{\text{ext}_2}$ evaluated at $r = R_2$. Using this one can write the GPE [Eq. (2.1)] as

$$-\frac{\nabla^2}{2}\psi_2 + (r - R_2)F\psi_2 + g_{22}|\psi_1|^2\psi_1 + g_{12}|\psi_1|^2\psi_2 = 0. \tag{4.2}$$

Introducing a dimensionless variable,

$$\xi_2 = \frac{r - R_2}{d_2}, \tag{4.3}$$

where,

$$d_2 = \left(\frac{1}{2F}\right)^{1/3},$$

(4.4)

gives d_2 as the distance from the classical radius R_2, where the Thomas-Fermi approximation starts failing. Upon introducing another dimensionless function ϕ_2 such that

$$\psi_2(r) = \alpha_2 \phi_2$$

(4.5)

where $\alpha_2 = (1/d)(1/2g_{22})^{1/2}$, one can write the GPE in terms of ϕ_2. Hence, the GPE takes the universal form

$$\phi_2'' - (\xi_2 + \phi_2^2)\phi_2 = 0,$$

(4.6)

where ϕ_2'' is the second order derivative of ϕ_2 with respect to ξ_2. Neglecting the non-linear term when $\xi_2 \to +\infty$, results in the equation simplifying to the form

$$\phi_2'' - \xi_2\phi_2 = 0,$$

(4.7)

the solution to which is an Airy function. The asymptotic behaviour then takes the form

$$\phi_2(\xi \to \infty) \simeq \frac{A}{2\sqrt{\pi}}\exp\left(-\frac{2}{3}\xi^{3/2}\right),$$

(4.8)

where A is a constant that can be numerically determined by matching Eq. (4.6) and Eq. (4.8), whose value is found to be $\simeq \sqrt{2}$ [28]. The solution hence takes the asymptotic form

$$\phi_2(\xi \to \infty) \simeq \frac{1}{\sqrt{2\pi}\xi^{1/4}}\exp\left(-\frac{2}{3}\xi^{3/2}\right),$$

(4.9)

giving the wave function as

$$\psi_2 = \frac{1}{\sqrt{2\pi}\xi^{1/4}}\exp\left(-\frac{2}{3}\xi^{3/2}\right)\alpha_2. \tag{4.10}$$

Near the inner boundary of the system, both components coexist. This is the boundary defined around R_1, which is the critical radius of that region. This is the boundary layer with both components coexisting on the inside and only component 2 on the outside [Fig. 4.2]. The Thomas-Fermi approximation starts failing near this critical radius. In order to include the contribution of the kinetic energy term in the GPE, first one needs to linearize the two potentials in the coupled equations for the two components around R_1,

$$V_{\text{ext}_1}(r) - \mu_1 \;=\; \frac{r^2}{2} - \mu_1 = \frac{R_1^2}{2} - \mu_1 + \frac{1}{2}(r - R_1), \tag{4.11}$$

$$V_{\text{ext}_2}(r) - \mu_2 \;=\; \frac{r^2}{2} - \mu_2 = \frac{R_1^2}{2} - \mu_2 + \frac{1}{2}(r - R_1). \tag{4.12}$$

This is followed by introducing the Thomas-Fermi equation for the second wave function into the equation for the first wave function and also introducing the Thomas-Fermi radius into the equation. The resulting equation describes the wave function as

$$\left[-\frac{\nabla^2}{2} + \left(1 - \frac{g_{12}}{g_{22}}\right)R_1(r - R_1) + g_{11}\Gamma_{12}|\psi_1|^2 \right]\psi_1 = 0. \tag{4.13}$$

Using the same method as that used for the outer boundary, one can write

$$V_{\text{ext}_1} - \mu_1 = (r - R_1)f. \tag{4.14}$$

42
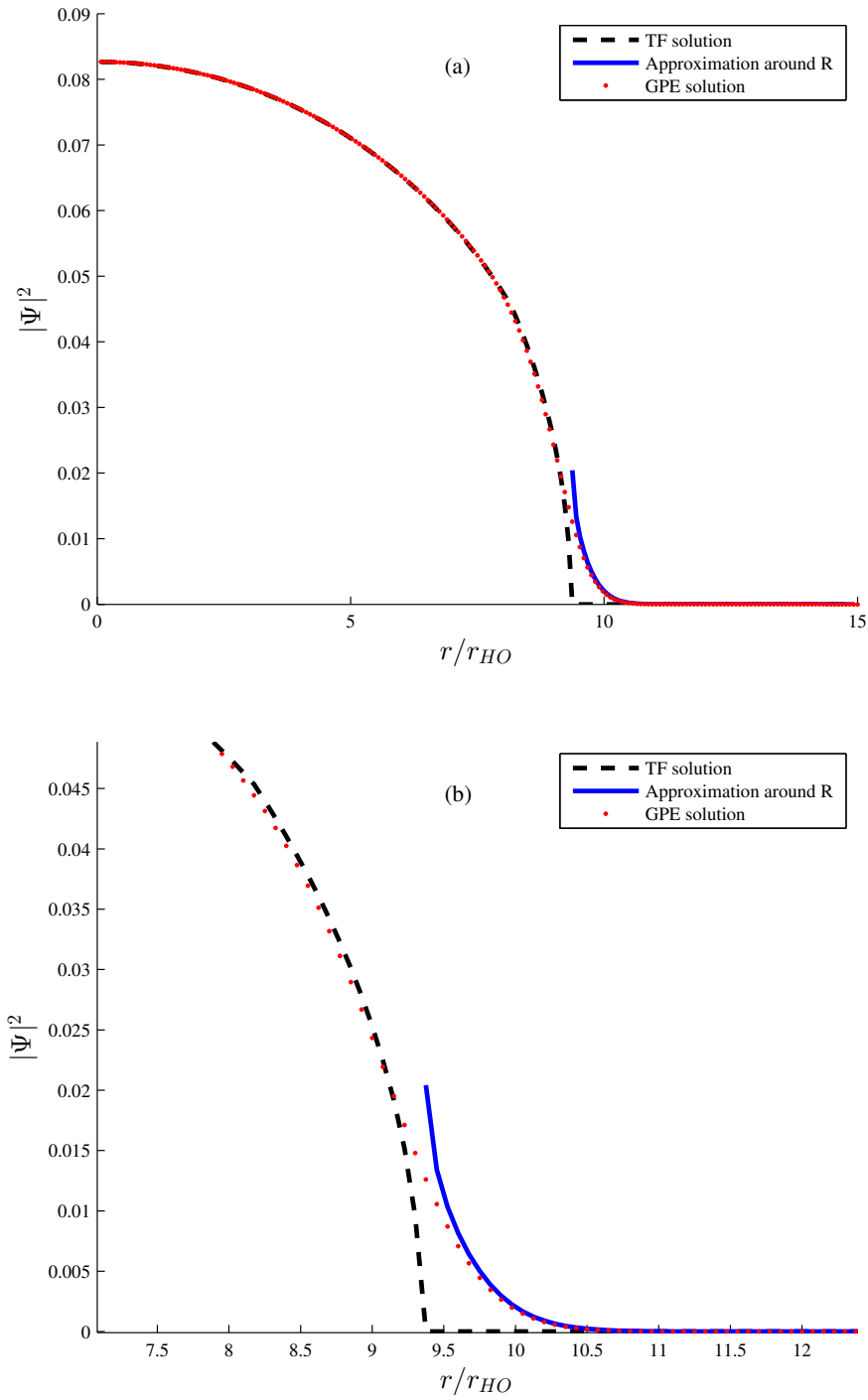
Figure 4.1: Fig:(a) plot showing the approximated solution to the universal equation [Eq. (4.10)], comparing with the GPE and TF solutions for a single component with the interaction strength as $g = 5000$; (b) Magnified image around the critical boundary.

One can therefore write

$$-\frac{1}{2}\frac{\partial^2 \psi_1}{\partial r^2} + (r - R_1)f\psi_1 + g_{12}\Gamma_{12}|\psi_1|^2\psi_1 = 0. \tag{4.15}$$

We then introduce a dimensionless variable

$$\xi_1 = \frac{r - R_1}{d_1}, \tag{4.16}$$

where,

$$d_1 = \left(\frac{1}{2f}\right)^{1/3} \tag{4.17}$$

is the thickness of the boundary from the critical radius R_1, and

$$f = R_1\left(1 - \frac{g_{12}}{g_{22}}\right). \tag{4.18}$$

We then introduce a dimensionless function ϕ_1, which is defined by

$$\psi_1 = \alpha_1\phi_1. \tag{4.19}$$

One can then write the GPE in terms of this dimensionless function, with it taking the universal form independent of the form of the external potential and the size of the inter-atomic forces,

$$\phi_1'' - (\xi_1 + \phi_1^2)\phi_1 = 0. \tag{4.20}$$
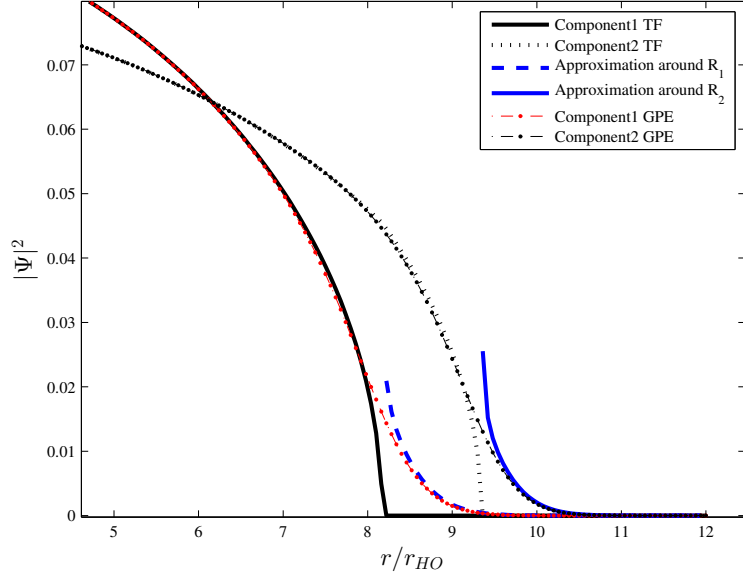
Figure 4.2: The solutions obtained from the universal equation [Eq. (4.20)] and the approximation of the Airy function, along with the GPE and TF solutions obtained numerically and analytically for the case when both components are disks, with $g_{11} = 3000$ and $g_{22} = 5000$ and their values of g_{12} as 1000.

4.2.2 Disk plus annulus

For the case when the value of g_{12} becomes greater than g_{12}^{ann} [Eq. (2.30)], the two-disks condensate now transitions into a disk plus annulus case according to the TF analysis. The TF solution around the region defined by the critical radius, R_2^-, is very sharp when compared to the GPE solution found numerically. This is partly due to neglecting the contribution of the kinetic energy term, which is significant around that region. Following the method described in the previous subsection (4.2.1), one can linearize the potential around R_2^- in the same way as was done for R_1 for the two disks case. This gives more accurate results when we compare it against the results obtained using the TF with the GPE solutions. For the disk plus annulus case there are three
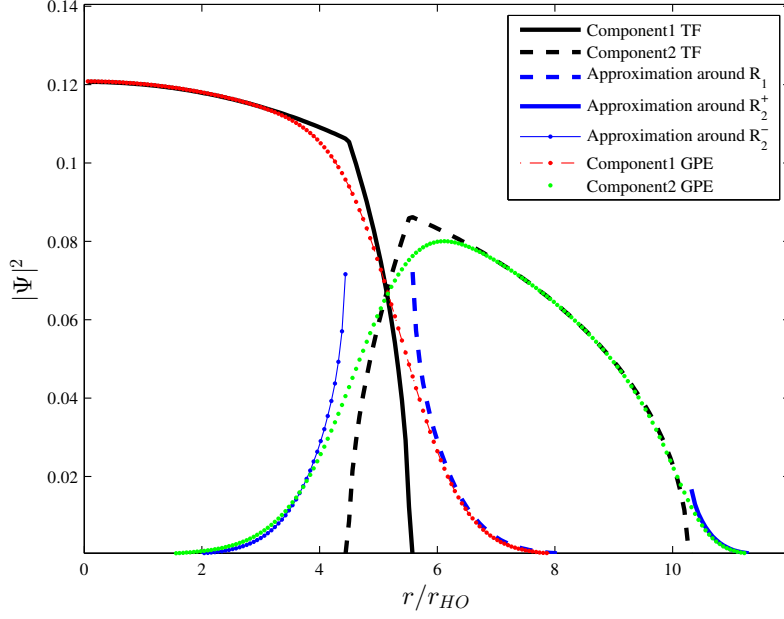
Figure 4.3: Plot showing the approximation of the Airy functional solution, the GPE solutions and the TF solutions for the disk plus annulus case, for all the three critical boundary regions, with $g_{11} = 3000$ and $g_{22} = 5000$ and the values of g_{12} as 3800.

critical radii, R_2^-, R_2^+, and R_1. The dimensionless variable ξ around R_2^- is

$$\xi_3 = -\left(\frac{r - R_2^-}{d_3}\right), \tag{4.21}$$

where the dimensionless variable d_3 is the same as d_1 [eq. (4.17)] and f is given by Eq. (4.18). Using these we can obtain the universal equation [Eq. (4.6)] and hence its solution in the form of an approximation of the Airy function [Eq. (4.8)]. Finally, we can obtain an approximated solution for the wavefunction around all the three critical radii [Fig. 4.3].

4.3 Generic case

In order to see which parameters actively affect the nature of the system, we now consider a more generic case with different masses ($m_1 \neq m_2$), number of particles ($N_1 \neq N_2$) and trapping frequencies ($\omega_1 \neq \omega_2$).

Consider the case where both the components are two disks and the GPE taking the radial form as

$$-\frac{\zeta \nabla^2 \psi_1}{2} - \frac{1}{r}\nabla\psi_1 + [V_{\text{ext}_1} - \mu_1]\psi_2 + g_{11}|\psi_1|^2\psi_1 + g_{12}\eta|\psi_2|^2\psi_1 = 0, \qquad (4.22)$$

for the first boundary, R_1, and

$$-\frac{\nabla^2 \psi_2}{2\zeta} - \frac{1}{r}\nabla\psi_2 + [V_{\text{ext}_2} - \mu_2]\psi_2 + g_{22}|\psi_2|^2\psi_2 + \frac{g_{12}}{\eta}|\psi_1|^2\psi_2 = 0, \qquad (4.23)$$

where

$$V_{\text{ext}_1} = \frac{r^2}{2\zeta\epsilon^2}, \qquad (4.24)$$

$$V_{\text{ext}_2} = \frac{\zeta\epsilon^2 r^2}{2}, \qquad (4.25)$$

We can then find the linear approximation following the method described in the previous subsection (4.2.1) and subsection (4.2.2). One hence arrives at the universal equation [Eq. (4.6)] for the general case, with the dimensionless variables as

$$d_2 = \left(\frac{1}{2F\zeta}\right)^{1/3}, \qquad (4.26)$$

47

where $F = \zeta \epsilon^2 R_2$, and

$$\alpha_2 = \frac{1}{d_2} \left(\frac{1}{2\zeta g_{22}} \right)^{1/2}. \tag{4.27}$$

Therefore, we obtain the universal equation [Eq. (4.6)] using Eq. (4.23), Eq. (4.26) and Eq. (4.27) for the generic case. One can regain the results obtained for the case with equal masses, equal particle numbers and equal trapping frequencies (subsection 4.2.1) and subsection 4.2.2) by setting $\zeta = 1$, $\eta = 1$ and $\epsilon = 1$. Similarly, for the two inner boundaries (around critical radii R_2^- and R_1), following the previously stated method (subsection (4.2.2)), one can find the universal equation for the generic case. For the boundary around R_1, the GPE with the linearized potential is

$$-\frac{\zeta \partial^2 \psi_1}{2\partial^2 r} + (r - R_1)f + |\psi_1|^2 \left(g_{11} - \frac{g_{12}^2}{\eta g_{22}} \right), \tag{4.28}$$

where,

$$f = R_1 \left(\frac{1}{\zeta \epsilon^2} - \frac{\zeta \epsilon^2 g_{12}}{g_{22}} \right). \tag{4.29}$$

Having redefined f and hence, Eq. (4.16) and Eq. (4.17), we arrive at the universal equation[Eq. (4.20)]. We follow the same procedure for the boundary defined by R_2^- for the disk plus annulus case, i.e. by defining the dimensionless variable d_3 as given by Eq. (4.21). Using this method of approximation one can find approximate solutions to a two-component BEC system, with parameters such as the masses, particle number, and trapping frequency that can be varied.

4.4 Analysis

The method of linearizing the potential and keeping in the Laplacian term implies the inclusion of the contribution of the kinetic energy to the system. Using this method and approximating the equation obtained to the form of a universal equation, one obtains the solution in the form of an approximation of the Airy function. This yields results which match with the numerics of the GPE. Even for values very close to the critical value where the Thomas-Fermi fails, this method of approximation works well when compared with the GPE solutions [Fig. 4.4, Fig. 4.5].

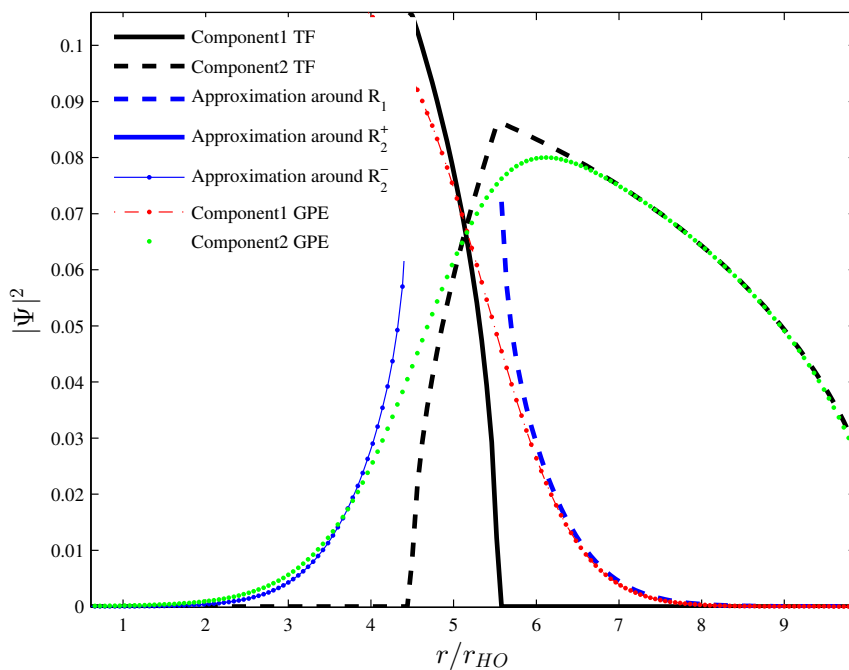Figure 4.4: A magnified view of the disk plus annulus case where one can see that the Airy function approximation does not completely agree with the GPE solution.

However, the approximation does not produce as good results for the innermost critical radius (around R_2^-) as it does for the two outer boundaries. This can be so because of a couple of factors. One of them is that the linearization of the potential
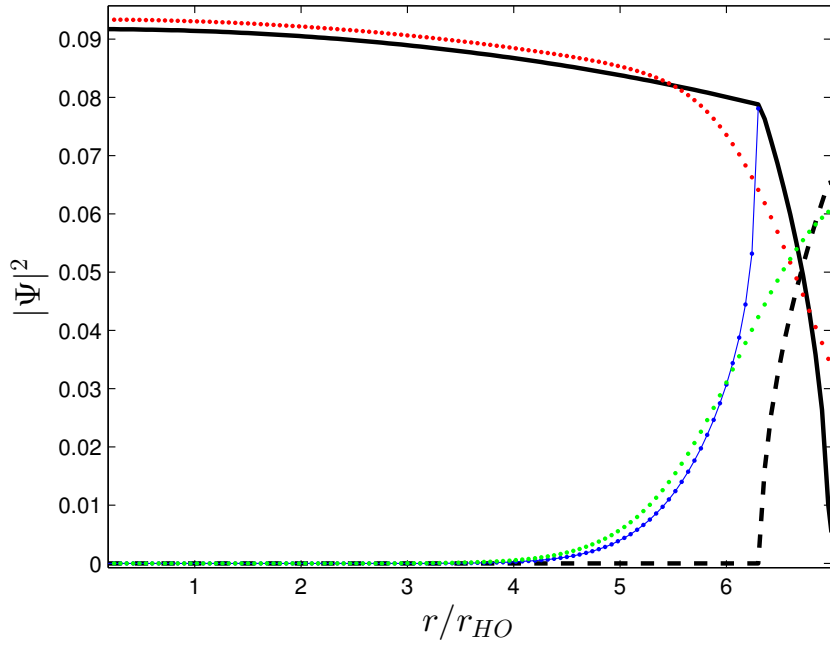
Figure 4.5: For higher values of interaction strengths, the approximation agrees with the GPE solutions. The figure shows the disk plus annulus case with values of $g_{11} = 9000$ and $g_{22} = 16000$ and the value of g_{12} as $\sqrt{0.98g_{11}g_{22}}$.

using the TF solution for defining all the radii and the chemical potentials is done so by neglecting the Laplacian term. But this fails as the solution tends towards the origin. The $1/r$ term from the Laplacian term tends to infinity as the solution tends to zero, which does not match with the asymptotic form of the solution.

In cases where the radius of the condensate is large, the Laplacian being neglected does not affect the solution to a great extent as it is far from the origin. The validity of the approximation follows from the assumption that the critical radius is far from the origin. This can generally be assumed to be always true for the two disks case within the mean-field approximation as the GPE solution tends towards infinity. However, this may not always be the case in the disk plus annulus regime, where the critical radius R_2^- may be far or close to the origin depending on the parameter regime, specifically,

the strength of the nonlinearity and the condition from transitioning from two-disk to disk plus annulus [Eq. (2.20)]. When the interaction strengths are large, one obtains better results. As the interaction strengths become large, the healing lengths become shorter and the shape of the wavefunction at R_2^- becomes taller and radially thinner [Fig. 4.6].
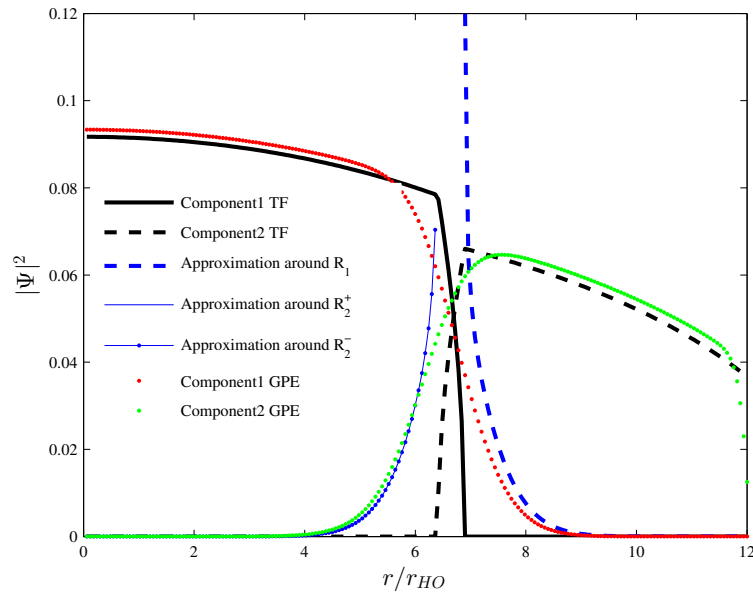
Figure 4.6: The figure shows the approximated solutions to the universal equation, the numerical GPE solutions and the TF solutions for two of the critical boundaries, with $g_{11} = 8000$ and $g_{22} = 16000$ and their values of g_{12} as $\sqrt{0.98 g_{11} g_{22}}$.

4.5 Dimensionality

The Gross-Pitaevskii equation describes the wave function of a Bose-Einstein Condensate system as a nonlinear Schrödinger equation. Experimentally, the two-component system is in a three dimensional trapping potential. However, it is advantageous to work in 2D and 1D in order to study the system under different parameters to get a

better understanding of the system. This is so because considering the system in 2D or 1D implies that the system now is axially or radially tight, respectively, relative to the other directions for a cylindrically symmetric configuration. The two-component GPE in 3D is expressed as

$$i\hbar \frac{\partial \psi_k}{\partial t} = \left(-\frac{\hbar^2 \nabla^2}{2m_k} + V_k(r) + U_k |\psi_k|^2 + U_{k,3-k} |\psi_{3-k}|^2 \right) \psi_k, \tag{4.30}$$

where $U_k = 4\pi \hbar^2 a_i / m$, are the intra-condensate interactions, and $U_{k,3-k} = 2\pi \hbar^2 a_{k,3-k}(m_k + m_{3-k})/(m_k m_{3-k})(k = 1, 2)$ is the inter-condensate interaction; m_k is the mass of a particle of each condensate; a_k, $a_{k,3-k}$ are the corresponding scattering lengths; and $V_k(r)$ are the external trapping potentials [19]. The trapping potential is defined as

$$V_k(r) = \frac{m_k \omega_{\text{radial}}^2 (x^2 + y^2)}{2} + \frac{m_k \omega_{\text{axial}}^2 z^2}{2}, \tag{4.31}$$

such that the trapping potentials differ in 1D and 2D based on $\omega_{\text{radial}} \gg \omega_{\text{axial}}$ and $\omega_{\text{axial}} \gg \omega_{\text{radial}}$, respectively. The interaction strengths in 2D and 1D differ from those in 3D by a factor such that,

$$U_{2D} = \frac{U_{3D}}{\sqrt{2\pi} a_\perp}, \tag{4.32}$$

$$U_{1D} = \frac{U_{3D}}{2\pi a_\perp^2}, \tag{4.33}$$

where $a_\perp = \sqrt{\hbar/m\omega_\perp}$ and $\omega_\perp$ refers to the transversal trapping frequency that reduces the dimensions into only axial frequencies in 2D and only radial frequencies in 1D [1].

In 2D, the intra-atomic and interatomic interaction strengths are $U_k = \sqrt{8\pi} \hbar^2 a_k / [m_k a_{zk}]$ and $U_{k,3-k} = \sqrt{2\pi} \hbar^2 a_{k,3-k} / [m_{k,3-k} \tilde{a}_z]$, respectively, with $m_{k,3-k}^{-1} = m_k^{-1} + m_{3-k}^{-1}$ as the re-

duced mass, and a_k and $a_{k,3-k}$ are the s-wave scattering lengths in the radial direction, a_{zk} it the characteristic size of the condensate in the z direction, and $\tilde{a}_z = (a_{z1} + a_{z2})/2$ [1, 19]. This is so due to the axial frequencies being considerably stronger than the radial frequencies and hence the wave function describing the system in the axial direction is considered to be of Gaussian form. While considering the system in 1D, the radial frequencies now become much stronger when compared to the axial frequencies. Using the Gaussian form of the radial wave function one obtains the interaction strength as $U_k = 2\hbar^2 a_k/m_k a_{\perp,k}^2$ where and $U_{k,3-k} = \hbar^2 a_k(m_k + m_{3-k})/\left(m_k m_{3-k} a_{\perp,k}^2\right)$ [1].

Developing on the theory stated in the previous subsections, there is a difference in the approximation with the change in dimensions. This is given through the change in the Laplacian term in one, two and three dimensions. In 1D, one only has the second derivative term [Eq. (3.5)] where as in 2D and 3D, one also has the radial term which is dependent on the first derivative with a pre-factor of $1/r$ or $1/r^2$[(Eq. (3.3) and Eq. (3.4)], respectively.

The approximation is based on the assumption that the critical radius R_2^- is far from the origin, which does not always hold true. Hence, the results do not completely comply with the GPE solutions for certain values of the interaction strengths. The factor that determines the compliance of the approximation is related to the strength of the nonlinearity and the condition for the transition from the two disks case to the disk plus annulus case (g_{12}^{ann}) (section 4.4).

Conclusions

The ground states in GPE treatment of a two-component Bose-Einstein system has been studied in detail in this thesis. BECs provide a large number of observable quantum mechanical effects and the way these effects present themselves depend on various parameters. These parameters are namely, the intercomponent and intracomponent interaction strengths of the two components, the particle numbers, the masses, and the trapping frequencies. Out of these parameters, the intercomponent and intracomponent strengths are the ones which determine whether the condensate mixture is in the form of two disks or is in the from of a disk plus an annulus. They are also a critical factor in determining phase separation in the condensate and its stability.

The Thomas-Fermi approximation helps determine the behaviour of the condensate as one varies these factors. This method of finding approximate solutions for finding ground states has been known to provide with reliable results. However, the solutions obtained become less reliable when compared to the exact GPE solutions as one gets further the Thomas-Fermi limit. This curbs its use as we get near the condition for phase separation. This is due to fact that the Thomas-Fermi approximation is based on the assumption that the kinetic energy term is negligible, which then no longer holds true.

In order to understand the system better, it is essential to come up with a more

accurate method of approximation. One such method which includes the nonlinear effects is suitably expanding the trapping potential term near the classical turning point. This gives us a more precise solution, even in different dimensionalities. This method too has its limitations. The approximation is not as good as one tends towards the origin and can be attributed to a number of reasons. One of these being that we consider the Thomas-Fermi solution as the initial guess, and the other being that we neglect the Laplacian term when working in 2D and 3D.

Finally, one might also use variational methods to find more accurate ground state solutions. One such method which provides with the scope of using variational analysis is the nonlinear σ model (see Appendix A), using which one can recover the ground states of a two-component condensate from the energy functional represented in terms of the total density and spin vector.

Appendix

Appendix A: Non-linear Sigma Model

TF Approach

One of the methods with which one can get the ground states of the stationary two-component condensate is the 'nonlinear σ model' [19] formulation of the energy functional in terms of the total density ρ_T and spin vector S_Z. This section analyzes the different Thomas-Fermi regimes using the nonlinear σ model. The coupled Gross-Pitaevskii equation in 2D can be written as

$$\mu_1 \psi_1 = \left[-\frac{\zeta \nabla^2}{2} + \frac{r^2}{2\zeta \epsilon^2} + \zeta g_{11} |\psi_1|^2 + \left(\frac{\zeta^2 + 1}{2\zeta} \right) g_{12} |\psi_2|^2 \right] \psi_1, \qquad \text{(A.1)}$$

$$\mu_2 \psi_2 = \left[-\frac{\nabla^2}{2\zeta} + \frac{r^2 \zeta \epsilon^2}{2} + \frac{g_{11}}{\zeta} |\psi_2|^2 + \left(\frac{\zeta^2 + 1}{2\zeta} \right) g_{12} |\psi_1|^2 \right] \psi_2. \qquad \text{(A.2)}$$

with $\zeta = \sqrt{m_2/m_1}$ and $\epsilon = \sqrt{\omega_2/\omega_1}$, with the normalization condition taken to be

$$\int |\psi_k|^2 \, d^2r = N_k, \qquad \text{(A.3)}$$

I

where N_k is the total particle number of the kth component, or

$$\int \left(|\psi_1|^2 + |\psi_2|^2 \right) d^2r = N_1 + N_2. \tag{A.4}$$

Hence the total density can be written as

$$\rho_T = |\psi_1|^2 + \frac{1}{\zeta^2}|\psi_2|^2 \tag{A.5}$$

The energy functional of the two wave functions can be written as $E[\psi_1, \psi_2] = E_{KE} + E_{PE} + E_I$, where

$$E_{KE} = \frac{\zeta^2}{\zeta^2 + 1} \int |\nabla\psi_1|^2 + \frac{1}{\zeta}|\psi_2|^2 \, d^2r, \tag{A.6}$$

$$E_{PE} = \int 2j_1 r^2 |\psi_1|^2 + 2j_2 r^2 |\psi_2|^2 \, d^2r, \tag{A.7}$$

$$E_I = \int \frac{1}{2}g_1|\psi_1|^4 + \frac{1}{2}g_2|\psi_2|^4 + g_{12}|\psi_1|^2|\psi_2|^2 \, d^2r. \tag{A.8}$$

with

$$j_1 = \frac{1}{2}\frac{(1 + 1/\zeta^2)}{(1 + \epsilon^2)^2}, \tag{A.9}$$

$$j_2 = \frac{1}{2}\frac{(1 + \zeta^2)}{\zeta^4(1 + 1/\epsilon^2)^2}. \tag{A.10}$$

We define a normalized complex-valued spinor $\chi = [\chi_1, \chi_2]^T$ from which the wave functions are decomposed as $\psi_1 = \sqrt{\rho_T}\chi_1, \psi_2 = \sqrt{\rho_T \zeta^2}\chi_2$, where $|\psi_1|^2 + |\psi_2|^2 = 1$. The spin density is defined as $S = \bar{\chi}\sigma\chi$, where σ are the Pauli matrices. This gives the

component of S as

$$S_x = \chi_1^* \chi_2 + \chi_2^* \chi_1, \tag{A.11}$$

$$S_y = -i(\chi_1^* \chi_2 - \chi_2^* \chi_1), \tag{A.12}$$

$$S_z = |\chi_1|^2 - |\chi_2|^2, \tag{A.13}$$

with $|S|^2 = 1$ everywhere. This gives us

$$|\psi_1| = \frac{1}{2}\rho_T(1 + S_z), |\psi_2|^2 = \frac{1\zeta^2}{2}\rho_T(1 - S_z). \tag{A.14}$$

We then define the phases θ_1 and θ_2 by $\chi_1 = |\chi_1| \exp(i\theta_1)$ and $\chi_2 = |\chi_2| \exp(i\theta_2)$. The energy functional can be expressed in terms of four variables: the total density ρ_T, the component S_z, and the angles θ_1 and θ_2. This gives us $E_{KE} = E_{\rho_T} + E_{S_z} + E_{\theta_1,\theta_2}$. E_{KE} at a constant phase can therefore be written as equal to $E_{\rho_T} + E_{S_z}$, where

$$E_{\rho_T} = \int \frac{\zeta^2}{(\zeta^2 + 1)}(\nabla \sqrt{\rho_t})^2 \, d^2r, \tag{A.15}$$

$$E_{S_z} = \int \frac{1}{4}\frac{\rho_T \zeta^2}{\zeta^2 + 1}\frac{(\nabla S_z)^2}{(1 - S_z^2)} \, d^2r. \tag{A.16}$$

The rest of the terms then become

$$E_{PE} = \int [(j_1 + j_2\zeta^2) + (j_1 + j_2\zeta^2)S_z]r^2\rho_T \, d^2r, \tag{A.17}$$

$$E_I = \int \frac{\rho_T^2}{2}(\bar{c}_0 + \bar{c}_1 S_z + \bar{c}_2 S_z^2) \, d^2r, \tag{A.18}$$

III

with

$$\bar{c}_0 = \frac{\zeta^4}{4}(g_{11}/\zeta^4 + g_{22} + 2/\zeta g_{12}), \tag{A.19}$$

$$\bar{c}_1 = \frac{\zeta^4}{2}(g_{11}/\zeta^4 - g_{22}), \tag{A.20}$$

$$\bar{c}_2 = \frac{\zeta^4}{4}(4g_{11}/\zeta^4 + g_{22} - 2\eta\gamma_{12}). \tag{A.21}$$

Hence the complete energy is

$$E = \int \frac{\zeta^2}{(\zeta^2 + 1)}(\nabla \sqrt{\rho_T})^2 + \frac{\rho_T \zeta^2}{4(\zeta^2 + 1)}\frac{(\nabla S_z)^2}{(1 - S_z^2)} + \frac{\rho_T \zeta^2}{2(1 + \zeta^2)}$$
$$+ [(j_1 + j_2\zeta^2) + (j_1 - j_2\zeta^2)S_z]r^2\rho_T + \frac{\rho_T^2}{2}(\bar{c}_0 + \bar{c}_1 S_z + \bar{c}_2 S_z^2)\, d^2r. \tag{A.22}$$

The energy (3.18) is subject to the constraints (1.2) that can be rewritten as

$$\int \rho_T \frac{(1 - S_z)}{2}d^2r = \frac{N_2}{\zeta^2}, \tag{A.23}$$

$$\int \rho_T S_z\, d^2r = N_1 - \frac{N_2}{\zeta^2}. \tag{A.24}$$

Under the Thomas-Fermi (TF) approximation we assume that the derivatives in ρ_T and S_z are negligible in front of the other terms. If we apply the TF approximation and minimize the energy under the constraints [Eq. (4.55) and Eq. (4.56)] we get

$$\mu + \lambda S_z = [(j_1 + j_2/\eta) + (j_1 - j_2\zeta^2)S_z]r^2 + \rho_T(\bar{c}_0 + \bar{c}_1 S_z + \bar{c}_2 S_z^2) \tag{A.25}$$

and

$$\lambda = (j_1 - j_2\zeta^2)r^2 + \frac{1}{2}(\bar{c}_1 + 2c_2 S_z)\rho_T. \tag{A.26}$$

IV

The TF energy is then

$$E_{TF} = \int ([(j_1 + j_2\zeta^2) + (j_1 - j_2\zeta)S_z]r^2 + \frac{\rho_T^2}{2}(\bar{c}_0 + \bar{c}_1 S_z + \bar{c}_2 S_z^2) - \mu\rho_T - \lambda\rho_T S_z)d^2r \quad \text{(A.27)}$$

Solving Eqs. 3.21 and 3.23 simultaneously for S_z and ρ_T we get

$$\rho_T = \frac{a_3 + a_4 r^2}{g_{11}g_{22}\Gamma_{12}} \quad \text{(A.28)}$$

and

$$S_z = \frac{a_1 + a_2 r^2}{a_3 + a_4 r^2} \quad \text{(A.29)}$$

where

$$a_1 = 4\frac{\lambda\bar{c}_0 - \mu\bar{c}_1/2}{\zeta^4} \quad \text{(A.30)}$$

$$a_2 = g_{11}h_2\zeta^2 - g_{22}h_1, \quad \text{(A.31)}$$

$$a_3 = 4\frac{\mu\bar{c}_2 - \lambda\bar{c}_1/2}{\zeta^4}, \quad \text{(A.32)}$$

$$a_4 = -(g_{11}h_2\zeta^2 + g_{22}h_1), \quad \text{(A.33)}$$

and where we define

$$h_k = 2\left(j_k - \frac{g_{12}}{g_{3-k}}j_{3-k}\right). \quad \text{(A.34)}$$

When only one component is present ($\psi_1 \times \psi_2 = 0$), this simplifies to

$$\rho_T = \begin{cases} \dfrac{1}{g_{11}}[\mu + \lambda - 2j_1 r^2], & \text{if}\,\psi_2 = 0 \\[2ex] \dfrac{\eta}{g_{22}}[(\mu - \lambda)/\zeta^2 - 2j_2 r^2,] & \text{if}\,\psi_1 = 0 \end{cases}$$

V

since $S_z = +1$ when $\psi_2 = 0$ and $S_z = -1$ when $\psi_1 = 0$.

Further scope

The interaction energy is proportional to the density as one reaches the critical limit for the interaction terms. Hence, the central assumption for the TF approach is no longer satisfied near the edge of the gas cloud where the condensate density goes to zero. Here, the TF approximation breaks down and the kinetic energy operator needs to be included in order to describe the behaviour near the edges realistically [29]. The method described in the previous subsection ("TF approach") can be used to go beyond the TF limit so that we get a more realistic picture. One could do this by performing a variational analysis on the nonlinear σ model. This can be approached by neglecting the $\nabla \rho_T$ term, however, now including the ∇S_z term since we now want to include the kinetic energy at the two condensate boundaries (valid for $\tilde{\Gamma}_{12} < \Gamma_{12} < 1$, where $\tilde{\Gamma}_{12}$ is some large and negative value we should look to calculate).

Figure 7: Thomas-Fermi solutions for different cases, from when both the components are disk shaped, transitioning to the disk plus annulus case; using Eq. (A.28) and Eq. (A.29). In all cases, $N_1 = N_2 = 1 = 10^4$, $g_1 = 1$, $g_2 = 2$, $\zeta = 2.337$, $\epsilon = 1.558$. Plots (a), (b) and (c) are cases with g_{12} as 0.5, 0.9 and 1.00.
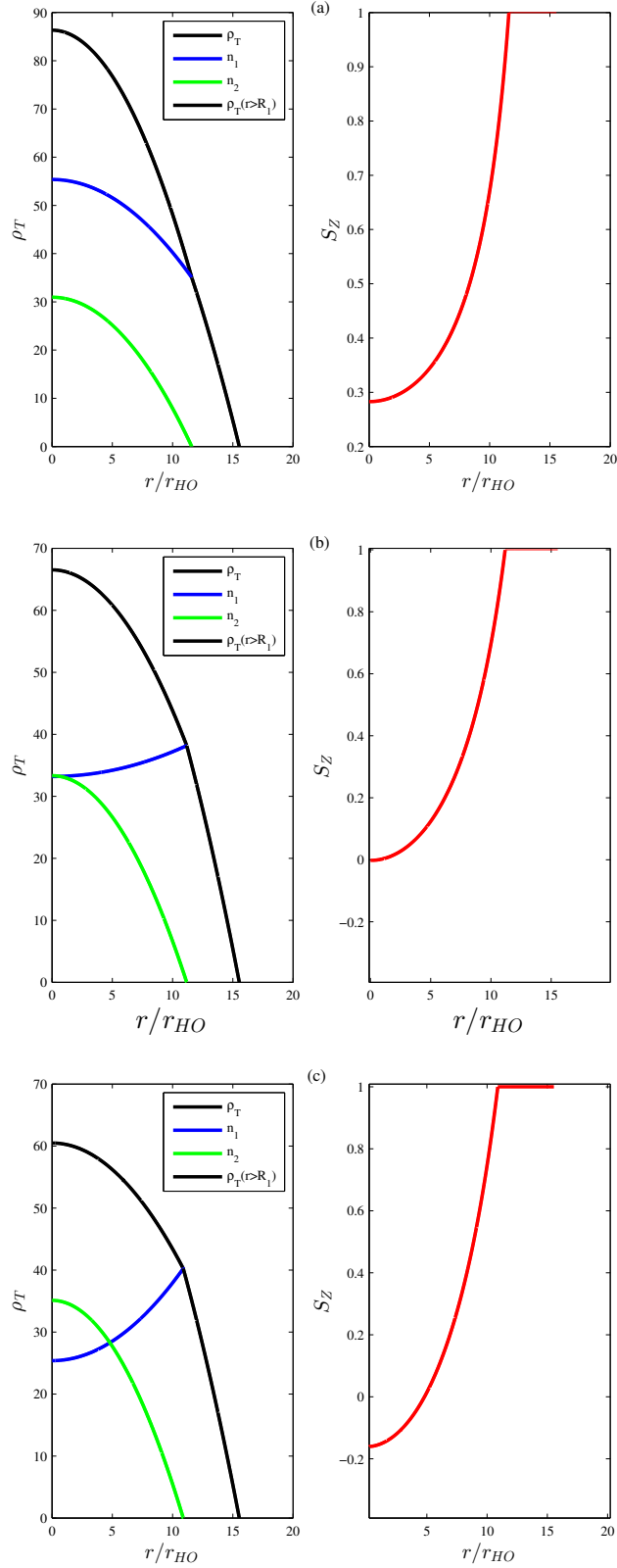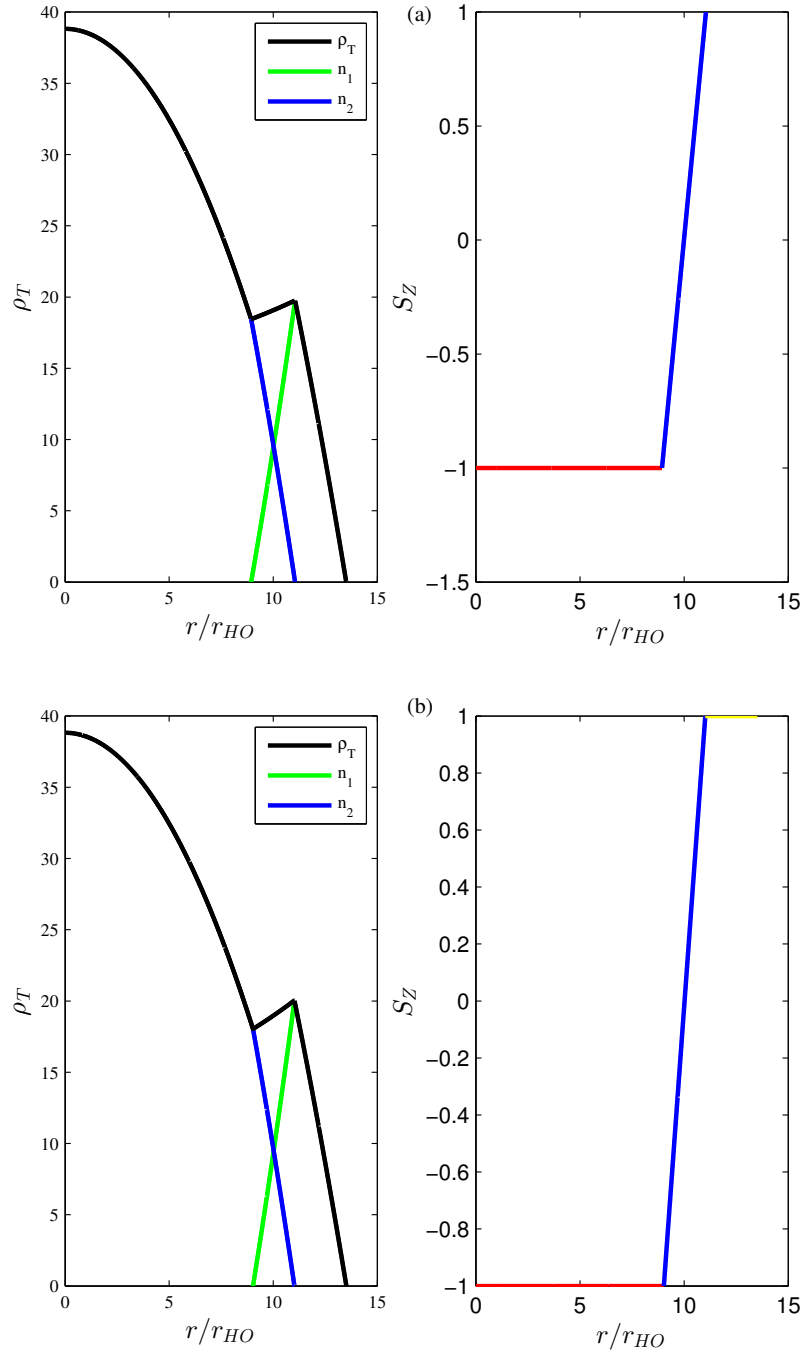
Figure 8: Thomas-Fermi solutions for different cases, from when both the components are disk shaped, transitioning to the disk plus annulus case; using Eq. (A.28) and Eq. (A.29). In all cases, $N_1 = N_2 = 10^4$, $g_1 = 1$, $g_2 = 1$, $\zeta = 2.337$, $\epsilon = 1.558$. Plots (a) and (b) are cases with g_{12} as 1.19 ($\simeq g_{12}^{\text{ann}}$), 1.20.

Appendix B: GPE Matlab Code

Evaluate G

```matlab
function [ G, Jac ] = evalG( X, V1, V2, r, g11, g22, g12,

N1, N2, d2matrix, delta_r )

%EVALG Evaluate the residual of a two-component GPE

%   X contains psi1=X(1:n) and psi2=X(n+1:2*n)

%   This function evaluates the residual, G, when psi1 and psi2 are fed into

%   the two-component GPE functional, the 'eigenvalues' are calculated, and

%   the eigenvalues times the wavefunctions are subtracted. If psi1 and

%   psi2 are a stationary (eigenvalue) solutions of the GPE, this residual

%   is equal to zero.

%   This function also reutrns the Jacobian matrix of derivatives of the

%   residual with respect to the grid-point values of the wavefunction (the

%   elements of psi1 and psi2). This information improves the performance

%   of fsolve significantly in most cases.

% Extract psi1 and psi2 from combined vector

s = size(X);

n = s(1)/2;

psi1 = X(1:n);

psi2 = X(n+1:2*n);


% Evaluate the GPE right hand side, getting 'eigenvalues' at the same time

[ G, mu1, mu2 ] = getG( psi1, psi2, V1, V2,

r, g11, g22, g12, N1, N2, d2matrix, delta_r, n );
```

```matlab
% Evaluate the Jacobian with respect to all grid point values

[ Jac ] = getJac( psi1, psi2, V1, V2,

r, g11, g22, g12, N1, N2, d2matrix, delta_r, mu1, mu2, n );

end
```

Jacobian matrix

```matlab
function [ Jac ] = getJac( psi1, psi2, V1, V2,

r, g11, g22, g12, N1, N2, d2matrix, delta_r, mu1, mu2, n )


%GETJAC Jacobian matrix for two-component GPE residual G

[dmu1_dj, dmu2_dj] = getDmuDj( psi1, psi2, V1, V2,

r, g11, g22, g12, N1, N2, d2matrix, delta_r );


Jac(1:n,1:n) = -(psi1*transpose(dmu1_dj)) ...

    - 0.5*d2matrix + diag(V1-mu1+(3*g11*psi1.^2+g12*psi2.^2));

Jac(n+1:2*n,n+1:2*n) = -(psi2*transpose(dmu2_dj)) ...

    - 0.5*d2matrix + diag(V2-mu2+(3*g22*psi2.^2+g12*psi1.^2));


Jac(1:n,n+1:2*n) = diag(2*g12*psi1.*psi2) ...

    - (psi1*2*delta_r*transpose(g12*psi1.^2.*psi2.*r)) *2*pi/N1;

Jac(n+1:2*n,1:n) = diag(2*g12*psi2.*psi1) ...

    - (psi2*2*delta_r*transpose(g12*psi2.^2.*psi1.*r)) *2*pi/N2;


end
```

X

Solve for G

```matlab
% --- Simple two-component GPE solver based on fsolve ---

%% Initialization of parameters and grid

% Initialize the grid for solving the problem

n = 200;

rmax = 12;

delta_r = rmax / n;

r = transpose(linspace(delta_r,rmax,n));


% Create a finite-difference second derivative matrix

d2matrix = full(gallery('tridiag',ones(1,n-1),-2*ones(1,n),ones(1,n-1)));

d2matrix(1,1) = -2/3;

d2matrix(1,2) = 2/3;

d2matrix = d2matrix /(delta_r^2);


d1matrix = (diag(ones(n-1,1),1)+diag(-ones(n-1,1),-1));

d1matrix(1,1) = -4/3;

d1matrix(1,2) = 4/3;

d1matrix = d1matrix / (2*delta_r);

d1matrix = diag(1./r)*d1matrix;


d2matrix = d2matrix + d1matrix;


%d2matrix = ( diag(-1.0*ones(1,n-2),-2) + diag(16.0*ones(1,n-1),-1) ...

% + diag(-30.0*ones(1,n),0) ...
```

```
% + diag(16.0*ones(1,n-1),1) + diag(-1.0*ones(1,n-2),2) ) /(12*delta_r^2);


% Set the nonlinearities
% Set values for the interaction strengths between different particles of
% the condensate component and the interaction strength between the two
% components of the condensate.
g11 = 3000;
g22 = 5000;
g12 =1000;
gm=1; %gamma=sqrt(m1/m2)


% Set the particle numbers
N1 = 1;
N2 = 1;


% Set the potentials
V1 = 0.5*r.^2;
V2 = 0.5*r.^2;


K=1; %w1/w2
beta1=1/K-(K*g12/g11);
beta2=1/K-(K*g12/g22);
gm12=1-((g12^2)/(g11*g22));
gcritical=sqrt(g11*g22);
%g12 for transition into disk plus annulus case
```

```matlab
ga12=N1*g11/2/(N1+N2) +(sqrt((g11^2*N1^2/(N1+N2)^2)+(4*N2*g11*g22/(N1+N2))))/2;


%% Set an initial guess for the wavefunctions


% --- NOTE ------------------------------------------------------
% It is important to start with a reasonably good initial guess for the
% ground state solution: if the initial guess is too distant from the
% ground state solution then the algorithm is likely to converge to an
% excited stationary state instead. Such excited states are easily
% identified by the appearance of nodes in the wavefunction.
% ---------------------------------------------------------------


% Set noninteracting ground states


%For the two disks case
%Calculating the Thomas-Fermi solutions
%Calculating the two critical radii and the chemical potentials


if g12<ga12 %condition for the two disks case
mu2=sqrt((N2*g22+N1*g12)/pi);
mu1=sqrt(N1*g11*gm12*beta2/pi)+(g12*mu2/g22);


R1=(4*N1*g11*gm12/pi/beta2)^0.25;
R2=(4*(N2*g22+N1*g12)/pi)^0.25;
```

```
%for the approximation around the different critical radii/ critical

%boundaries

%Calculating the dimenisonless quantities for the two components

%for the first component

%penetration depth

f=(1 - (g12/g22))*R1;

d1=(1/2/f)^(1/3);

alpha1=sqrt(1/2/g11/gm12)/d1;


%for the second component

F=K*R2;

d2=(1/(2*gm*F))^(1/3);

alpha2=sqrt(1/2/gm/g22)/d2;


[psi1a,psi2a]=thomasFermi(g11,g22,g12,gm12,K,mu1,mu2,R1,r );


[psi1b,psi2b]=thomasFermi1(g22,K,mu2,R1,R2,r );


psi1=psi1a+psi1b;

psi2=psi2a+psi2b;


[ xi1,taila ] = tail1( r,R1,d1,alpha1,rmax );

[ xi2,tailb ] = tail2( r,R2,d2,alpha2,rmax );
```

```matlab
else %Condition for the disk plus annulus case


%Calculating the Thomas-Fermi solutions for the disk plus annulus case

%Calculating the three critical radii and the two chemical potentials for

%the two components



mu1=sqrt(g11*(N1+N2)/pi);

mu2=mu1 +sqrt(-g11*g22*beta1*beta2*N2/pi/g12);



R2p=sqrt(2*(sqrt(g11*(N1+N2)/pi)+sqrt(-g11*g22*beta1*beta2*N2/pi/g12)));

R2n=sqrt(2*(sqrt(g11*(N1+N2)/pi)-sqrt(-g11*g22*beta2*N2/pi/g12/beta1)));

R1= sqrt(2*(sqrt(g11*(N1+N2)/pi)-sqrt(-g11*g12*beta1*N2/pi/g22/beta2)));



%Calculating the dimenisonless quantities for the two components

%for the first component

%penetration depth

f=(1 - (g12/g22))*R1;

d1=(1/2/f)^(1/3);

alpha1=sqrt(1/2/g11/gm12)/d1;



%for the second component

F=K*R2p;

d2=(1/(2*gm*F))^(1/3);

alpha2=sqrt(1/2/gm/g22)/d2;
```

```matlab
[psi1a,psi2a]=annulus1(mu1,r,K,g11,R2n );

[ psi1b,psi2b] = annulus2( mu1,mu2,g11,g22,g12,gm12,K,r,R2n,R1 );

[ psi1c,psi2c] = annulus3( r,R1,R2p,mu2,K,g22 );

psi1=psi1a+psi1b+psi1c;

psi2=psi2a+psi2b+psi2c;

[ xi1,taila ] = tail1( r,R1,d1,alpha1,rmax );

[ xi2,tailb ] = tail4( r,R2p,d2,alpha2,rmax );

[ xi3,tailc ] = tail3( r,R2n,d1,alpha1,rmax );

end
%% Solve equation
%Plot initial guess
figure(1);
clf;
plot(r,psi1/N1,'k'),xlabel('$r/r_{HO}$','Interpreter','LaTeX','FontSize',16),
ylabel('${\arrowvert\Psi\arrowvert^2}$','Interpreter','LaTeX','FontSize',16) ;
hold on;
plot(r,psi2/N2,'--k');
%plot approximated solution to the universal equation
%plot(r,taila,'--b');
%plot(r,tailb,'b');


%if g12>ga12
%plot(r,tailc,'.-b');
%end
```

```matlab
% Pack psi1 and psi2 into the X0 vector required by fsolve

X0 = [psi1; psi2];


% Set the options for fsolve

%jopts = optimoptions('fsolve','jacobian','on','Display',

'iter','DerivativeCheck','on','MaxIter',4000);

jopts = optimset('jacobian','on','Display',

'iter','DerivativeCheck','on','MaxIter',4000);

% Run fsolve, calling the function evalG...

X = fsolve(@(X) evalG(X,V1,V2,r,g11,g22,g12,N1,N2,d2matrix,delta_r),X0,jopts);

% Unpack psi1 and psi2 from the X vector returned by fsolve

psi1 = X(1:n);

psi2 = X(n+1:2*n);


% Plot numerical solution

%plot(r,psi1,'.r');

%plot(r,psi2,'.b');

%legend('Component1 TF', 'Component2 TF', 'Approximation around R2',

'Approximation around R2','Copmonent1 GPE', 'Component2 GPE');
```

Evaluate derivative of the chemical potential μ_j with respect to ψ_j

```matlab
function [ dmu1_dj, dmu2_dj ] = getDmuDj( psi1, psi2, V1, V2,

 r, g11, g22, g12, N1, N2, d2matrix, delta_r )

%GETDMUDJ Derivative of eigenvalue mu with respect to psi_j

dmu1_dj = delta_r * ( ( -0.5*d2matrix*psi1 + 2*V1.*psi1 + ...
```

```
(4*g11*psi1.^3 +2*g12*psi2.^2.*psi1) ).*r

-0.5*transpose(d2matrix)*(psi1.*r) ) * 2*pi/N1;

dmu2_dj = delta_r * ( ( -0.5*d2matrix*psi2 + 2*V2.*psi2 + ...

(4*g22*psi2.^3 +2*g12*psi1.^2.*psi2) ).*r

-0.5*transpose(d2matrix)*(psi2.*r) ) * 2*pi/N2;

end
```

Two-component GPE residue for ψ_1 and ψ_2

```
function [ G, mu1, mu2 ] = getG( psi1, psi2, V1, V2,

r, g11, g22, g12, N1, N2, d2matrix, delta_r, n )

%GETG Two-component GPE residual for psi1, psi2

G1 = -0.5*d2matrix * psi1 + (V1 + (g11*psi1.^2 + g12*psi2.^2)).*psi1;

G2 = -0.5*d2matrix * psi2 + (V2 + (g22*psi2.^2 + g12*psi1.^2)).*psi2;

mu1 = delta_r * sum(psi1.*G1.*r) * 2*pi/N1;

mu2 = delta_r * sum(psi2.*G2.*r) * 2*pi/N2;

G1 = G1 - mu1.*psi1;

G2 = G2 - mu2.*psi2;

G = [G1; G2];

end
```

Solving for the linear approximations around the critical radii

Around R_2 for two disks or R_2^+ for disk plus annulus:

```
function [ xi1,taila ] = tail1( r,R1,d1,alpha1,rmax )

%Calculate the tail of the second component

% Using the Dalfovo method
```

```
    xi1=((r-R1)/d1).*(r>R1).*(r<rmax);

    taila=exp(-2/3.*(xi1.^1.5))*alpha1/sqrt(pi*2)./xi1.^0.25;

end
```

Around R_1 for both cases:

```
function [ xi2,tailb ] = tail2( r,R2,d2,alpha2,rmax )

%Calculate the tail of the second component

% Using the Dalfovo method

    xi2=(r-R2)/d2.*(r>R2).*(r<(rmax));

    tailb=exp(-2/3.*xi2.^1.5)*alpha2/sqrt(pi*2)./xi2.^0.25;

end
```

Around R_2^- for disk plus annulus:

```
function [ xi3,tailc ] = tail3( r,R2n,d1,alpha1,rmax )

%Calculate the tail of the second component

% Using the Dalfovo method

    xi3=(-(r-R2n)/d1).*(r>0).*(r<R2n);

    tailc=exp(-2/3.*(xi3.^1.5))*alpha1/sqrt(pi*2)./xi3.^0.25;

end
```

Around R_2^+ for disk plus annulus:

```
function [ xi2,tailb ] = tail4( r,R2p,d2,alpha2,rmax )

%Calculate the tail of the second component

% Using the Dalfovo method

    xi2=(r-R2p)/d2.*(r>R2p).*(r<(rmax));

    tailb=exp(-2/3.*xi2.^1.5)*alpha2/sqrt(pi*2)./xi2.^0.25;

end
```

Appendix C: Nonlinear σ Model Code

```
%Dispersion relationship for two-component condensate with v1 and v2


%Clear all variables and reset the form

clear all

clf

close all

format long g


%Define parameters

hbar=1.05457126*10^(-34);

a0=5.29*10^(-11);

u=1.660538921*10^(-27);

w1=2*pi*32.2; %v1(r)

w2=2*pi*40.2; %v2(r)

wz1=2*pi*3.89; %omega1

wz2=2*pi*4.55; %omega2

xi=w1/w2;

%xi=1/xi;

a1=100*a0; %scattering lengths

a2=280*a0;

a12=650*a0;

m1=86.930408*u;

m2=132.905451933*u;

eta=m1/m2;
```

```
%eta=1/eta;

m12i=1/m1+1/m2;

m12=1/m12i;

az1=sqrt(hbar/m1/wz1);

az2=sqrt(hbar/m2/wz2);

aztilde=0.5*(az1+az2);

N1=1*10^4; %particle numbers

N2=1*10^4;


%g

g1=1;

g2=2;

g12=1.19;

gam12=1-(g12^2/g1/g2);

%Trapping potential

V1=(eta+1)*xi^2/(xi+1)^2; % effective trapping potentials

V2=(eta+1)/eta/(xi+1)^2;

%factor=(1/eta/xi/xi)^2;

%g2

%g1*factor

j1=(1/2)*(1+eta)*xi^2/(1+xi)^2;

j2=(1/2)*(1+eta)/eta/(1+xi)^2;

c0=(eta^2*g1+g2+2*eta*g12)/4/eta^2;

c1=(eta^2*g1-g2)/2/eta^2;

c2=(eta^2*g1+g2-2*eta*g12)/4/eta^2;
```

```
y1=(1+eta)/(2*eta*(1+xi)^2);

gam1=2*y1*(1-(eta*xi^2*g12/g1));

gam2=2*y1*(eta*xi^2-g12/g2);

h1=2*(j1-g12*j2/g2);

h2=2*(j2-g12*j1/g1);

lam1=(j1/j2)^2;

lam2=(j2/j1)^2;

%ga12

if g2>(g1*lam2)

 ga12=N1*g1*j2/2/(N1*j1+N2*j2) +...

    0.5*sqrt(g1^2*N1^2*j2^2/(N1*j1+N2*j2)^2 + (4*N2*g1*g2*j2/(N1*j1+N2*j2)));

else

ga12=N2*g2*j1/2/(N1*j1+N2*j2) +...

    0.5*sqrt(g2^2*N2^2*j1^2/(N1*j1+N2*j2)^2 + (4*N1*g1*g2*j1/(N1*j1+N2*j2)));

end


%For calculating the total density and Sz.

%For calculating new mu1 and mu2

%For two disks

if g12<ga12

if g2<(g1*lam2)%R1>R2

R2=(2*N2*g2*gam12/pi/gam1)^(1/4);

R1=((N1*g1+N2*g2)/pi/(eta*xi^2*y1))^(1/4);

mu1=sqrt(4*eta*xi^2*y1/pi*(N1*g1+N2*g2));

mu2=g12*mu1/g1+sqrt(2*N2*g2*gam12/pi*gam1);
```

```
mu=(mu1+mu2/eta)/2;

lambda=(mu1-mu2/eta)/2;

a1=4*eta^2*(lambda*c0-mu*c1/2);

a2=eta*g1*h2-g2*h1;

a3=4*eta^2*(mu*c2-lambda*c1/2);

a4=-(eta*g1*h2+g2*h1);


%For calculating rho(total) and Sz1

r1=0:0.001:R2;

for i=1:length(r1)

rho1(i)=(a3+a4*(r1(i)^2))/(g1*g2*gam12);

Sz1(i)=(a1+a2*(r1(i)^2))/(a3+a4*(r1(i)^2));

n1a(i)=(mu1-g12*mu2/g2-gam2*r1(i)^2)/g1/gam12;

n2a(i)=eta*(mu2-g12*mu1/g1-gam1*r1(i)^2)/g2/gam12;

nt1(i)=n1a(i)+n2a(i);

end

subplot(1,2,1)

plot (r1,rho1,'k')

xlabel('$r/r_{HO}$','Interpreter','LaTeX','FontSize',16);

ylabel('$\rho_T$','Interpreter','LaTeX','FontSize',16);

hold on

plot(r1,n1a,'b')

hold on

plot(r1,n2a,'g')

hold on
```

```matlab
subplot(1,2,2)

plot(r1,Sz1,'r')

xlabel('$r/r_{HO}$','Interpreter','LaTeX','FontSize',16);

 ylabel('$S_Z$','Interpreter','LaTeX','FontSize',16);

hold on


r2=R2:0.001:R1;

for j=1:length(r2)

    rho2(j)=1/g1*(mu+lambda-2*j1*r2(j)^2);

    Sz2(j)=1;

  % n1b=(mu1-gam2*r1(j)^2)/g1;

 %  n2b=0;

  % nt2(j)=n1b(j)+n2b(j);

end

subplot(1,2,1)

plot(r2,rho2,'k')

hold on

subplot(1,2,2)

plot(r2,Sz2,'r')


else %(R2>R1)


R2=((N2*g2+N1*g12)/pi/y1)^(1/4);

R1=(2*N1*g1*gam12/pi/gam2)^(1/4);

mu2=sqrt(4*y1*(N2*g2+N1*g12)/pi);
```

```
mu1=(g12*mu2/g2) +sqrt(2*N1*g1*gam12*gam2/pi);

    mu=(mu1+mu2/eta)/2;

    lambda=(mu1-mu2/eta)/2;

    a1=4*eta^2*(lambda*c0-mu*c1/2);

    a2=eta*g1*h2-g2*h1;

    a3=4*eta^2*(mu*c2-lambda*c1/2);

    a4=-(eta*g1*h2+g2*h1);


    r1=0:0.001:R1;

    for i=1:length(r1)

    rho1(i)=(a3+a4*(r1(i)^2))/(g1*g2*gam12);

    Sz1(i)=(a1+a2*(r1(i)^2))/(a3+a4*(r1(i)^2));

    n1a(i)=(mu1-g12*mu2/g2-gam2*r1(i)^2)/g1/gam12;

    n2a(i)=eta*(mu2-g12*mu1/g1-gam1*r1(i)^2)/g2/gam12;

    nt1(i)=n1a(i)+n2a(i);

    end
subplot(1,2,1)
plot (r1,rho1,'k')
hold on
plot(r1,n1a,'r')
hold on
plot(r1,n2a,'g')
hold on
plot(r1,nt1,'r')
hold on
```

```
subplot(1,2,2)

plot(r1,Sz1,'r')

hold on


    r2=R1:0.001:R2;

 for j=1:length(r2)

   rho2(j)=eta/g2*(eta*(mu-lambda)-2*j2*r2(j)^2);

   Sz2(j)=-1;

   n1b(j)=0;

   n2b(j)=(mu2-gam1*r1(j)^2)/g2;

   nt2(j)=n1b(j)+n2b(j);

end

subplot(1,2,1)

plot(r2,rho2)

hold on

subplot(1,2,2)

plot(r2,Sz2,'r')

end

end


%For disk plus annulus case

 if g12>ga12

 %annulus in component 1

    if g2<(g1*lam2)

    R1p=(sqrt(g2/pi)/j2*((N1*j1+N2*j2)^(1/2)
```

```matlab
+(-g1*N1*h1*h2/4/pi/g12/j1)^(1/2)))^(1/2);

R1n=(sqrt(g2/pi)/j2*((N1*j1+N2*j2)^(1/2)

-(-g1*N1*j1*h2/pi/g12/h1)^(1/2)))^(1/2);

R2 =(sqrt(g2/pi)/j2*((N1*j1+N2*j2)^(1/2)

-(-j1*g12*h1*N1/pi/g1/h2)^(1/2)))^(1/2);

mu1=(sqrt(g2/pi)/j2*(2*j1*(N1*j1+N2*j2)^(1/2)

+(-j1*g1*h1*h2*N1/pi/g12)^(1/2)));

mu2=(4*g2/pi*(N1*j1+N2*j2))^(1/2);

mu=(mu1+mu2/eta)/2;

lambda=(mu1-mu2/eta)/2;

a1=4*eta^2*(lambda*c0-mu*c1/2);

a2=eta*g1*h2-g2*h1;

a3=4*eta^2*(mu*c2-lambda*c1/2);

a4=-(eta*g1*h2+g2*h1);

r1=0:0.001:R1n;

    for i=1:length(r1)

    rho1(i)=eta/g2*(eta*(mu-lambda)-2*j2*r1(i)^2);

    Sz1(i)=-1;

    n1a(i)=0;

    n2a(i)=eta*(mu2-2*j2*r1(i)^2)/g2;

    nt1(i)=n1a(i)+n2a(i);

    end

    subplot(1,2,1)

%plot (r1,rho1,'k',r1,n2a)

plot (r1,rho1,'k')
```

```matlab
xlabel('$r/r_{HO}$','Interpreter','LaTeX','FontSize',16);

ylabel('$\rho_T$','Interpreter','LaTeX','FontSize',16);

hold on

%plot(r1,n1a,'b')

%hold on

%plot(r1,n2a,'g')

%hold on

subplot(1,2,2)

plot(r1,Sz1,'r')

xlabel('$r/r_{HO}$','Interpreter','LaTeX','FontSize',16);

ylabel('$S_Z$','Interpreter','LaTeX','FontSize',16)


hold on

    r2=R1n:0.001:R2;

    for j=1:length(r2)

        rho2(j)=(a3+a4*(r2(j)^2))/(g1*g2*gam12);

        Sz2(j)=(a1+a2*(r2(j)^2))/(a3+a4*(r2(j)^2));

        SZ2(j)=(2/(R2-R1n))*r2(j)-(1+2*R1n/(R2-R1n)); %linear line equation

        n1b(j)=(mu1-g12*mu2/g2-gam2*r2(j)^2)/g1/gam12;

        n2b(j)=eta*(mu2-g12*mu1/g1-gam1*r2(j)^2)/g2/gam12;

        nt2(j)=n1b(j)+n2b(j);

    end

subplot(1,2,1)

%plot(r2,rho2,'r',r2,n1b,r2,n2b)

plot(r2,n1b,'g',r2,n2b,'b')
```

XXVIII

```
hold on

plot(r2,rho2,'k')

hold on

subplot(1,2,2)

plot(r2,Sz2,'r',r2,SZ2,'b')

hold on

    r3=R2:0.001:R1p;

    for k=1:length(r3)

        rho3(k)=1/g1*(mu+lambda-2*j1*r3(k)^2);

        Sz3(k)=1;

        n1c(k)=(mu1-2*j1*r3(k)^2)/g1;

        n2c(k)=0;

        nt3(k)=n1c(k)+n2c(k);

    end

subplot(1,2,1)

%plot(r3,rho3,r3,n1c)

plot(r3,rho3,'k')

hold on

%plot(r3,n1c,'b')

legend('\rho_T','n_1','n_2')

subplot(1,2,2)

plot(r3,Sz3,'y')


    else

%annulus in component 2
```

```
%if (g2*lam2)>g1

    R2p=sqrt(1/j1*sqrt(g1/pi)*((N1*j1+N2*j2)^(1/2)

    +(-g2*N2*h1*h2/4/pi/g12/j2)^(1/2)));

    R2n=sqrt(1/j1*sqrt(g1/pi)*((N1*j1+N2*j2)^(1/2)

     -(-g2*N2*h1*j2/pi/g12/h2)^(1/2)));

    R1 =sqrt(1/j1*sqrt(g1/pi)*((N1*j1+N2*j2)^(1/2)

     -(-g12*N2*h2*j2/pi/g2/h1)^(1/2)));

    mu2=1/j1*sqrt(g1/pi)*(2*j2*(N1*j1+N2*j2)^(1/2)

    +(-g2*N2*h1*h2/pi/g12*j2)^(1/2));

    mu1=(4*g1/pi*(N1*j1+N2*j2))^(1/2);

    mu=(mu1+mu2/eta)/2;

    lambda=(mu1-mu2/eta)/2;

    a1=4*eta^2*(lambda*c0-mu*c1/2);

    a2=eta*g1*h2-g2*h1;

    a3=4*eta^2*(mu*c2-lambda*c1/2);

    a4=-(eta*g1*h2+g2*h1);


    r1=0:0.001:R2n;

    for i=1:length(r1)

        rho1(i)=1/g1*(mu+lambda-2*j1*r1(i)^2);

        Sz1(i)=1;

        n1a(i)=(mu1-2*j1*r1(i)^2)/g1;

        n2a(i)=0;

        nt1(i)=n1a(i)+n1a(i);

    end
```

```matlab
    subplot(1,2,1)

    plot (r1,rho1,'k')

hold on

subplot(1,2,2)

plot(r1,Sz1,'r')

hold on

    r2=R2n:0.001:R1;

for j=1:length(r2)

    rho2(j)=(a3+a4*(r2(j)^2))/(g1*g2*gam12);

    Sz2(j)=(a1+a2*(r2(j)^2))/(a3+a4*(r2(j)^2));

    n1b(j)=(mu1-g12*mu2/g2-gam2*r2(j)^2)/g1/gam12;

    n2b(j)=eta*(mu2-g12*mu1/g1-gam1*r2(j)^2)/g2/gam12;

    nt2(j)=n1b(j)+n2b(j);

end

    subplot(1,2,1)

%plot(r2,rho2,'r',r2,n1b,r2,n2b)

plot(r2,n1b,'g',r2,n2b,'b')

hold on

plot(r2,rho2,'k')

hold on

subplot(1,2,2)

plot(r2,Sz2,'r')

hold on

    r3=R1:0.001:R2p;

    for k=1:length(r3)
```

```
        rho3(k)=eta/g2*(eta*(mu-lambda)-2*j2*r3(k)^2);

        Sz3(k)=-1;

        n1c(k)=0;

        n2c(k)=eta*(mu2-2*j2*r3(k)^2)/g2;

        nt3(k)=n1c(k)+n2c(k);

    end

    subplot(1,2,1)

%plot(r3,rho3,r3,n1c)

plot(r3,rho3,'r')

hold on

subplot(1,2,2)

plot(r3,Sz3,'y')

    end

  end
```

References

[1] L. Pitaevskii and S. Stringari. *Bose-Einstein Condensation*. 2003.

[2] C. J. Pethick and H. Smith. *Bose-Einstein Condensation in Dilute Gases*. 2003.

[3] A. Einstein. *Sitzungsber Preuss. Akad. Wiss. Bercht 3*, 1925.

[4] S. N. Bose. *Z. Phys. 26,178*, 1924.

[5] P. I. Kapitza. *Nature 141*, (74), 1938.

[6] Henk T.C. Stoof, Koos B. Gubbels, and Dennis B.M. Dickerscheid. *Ultracold Quantum Fields*. 2009.

[7] M. H. Anderson, M.R. Matthews J.R. Ensher, Eric Cornell, and Carl Wienman. Observation of Bose-Einstein Condensation in a Dilute Atomic Vapor. *Science*, 269, 1995.

[8] D. M. Stamper-Kurn, M. R. Andrews, A. P. Chikkatur, S. Inouye, J. Stenger H. J. Miesner, and W. Ketterle. Optical Confinement of a Bose- Einstein Condensate. *Phys. Rev. Lett.*, 80(10), 1998.

[9] C. C. Bradley, C. A. Sackett, J. J. Tollett, and R. G. Hulet. Evidence of Bose-

Einstein Condensation in an Atomic Gas with Attractive Interactions. *Phys. Rev. Lett.*, 75(9), 1995.

[10] G. Modugno, G. Ferrari, G. Roati, R.J. Brecha, A. Simoni, and M. Inguscio. Bose- Einstein Condensation of Potassium Atoms by Sympathetic Cooling. *Science 294*, (1320), 2001.

[11] K. B. Davis, M. O. Mewes, N. J. van Druten, D. S. Durfer, D. M. Kurn, and W. Ketterle. Bose Einstein Condensate in a Gas of Sodium Atoms. *Phys. Rev. Lett.*, 75(22), 1995.

[12] C. J. Myatt, E. A. Burt, R. W. Ghrist, E. A. Cornell, and C. E. Wieman. Production of two overlapping Bose-Einstein Condensates by Sympathetic Cooling. *Phys. Rev. Lett.*, 78(4), 1997.

[13] F. Perreira Dos Santos, J. Leonard, Junmin Wang, C. J. Barrelet, F. Perales, E. Rasel, C. S. Unnikrishnan, M. Leduc, and C. Cohen-Tannoudji. Bose- Einstein Condensation of Metastable Helium. *Phys. Rev. Lett.*, 86(3459), 2001.

[14] Tin-Lun Ho and V. B. Shenoy. Binary Mixtures of Bose Condensates of Alkali Atoms. *Phys. Rev. Lett.*, 117(16), 1998.

[15] D. S. Hall, J. R. Ensher, D. S. Jin, M. R. Matthews, C. E. Wieman, and E. A. Cornell. Recent Experiments with Bose- Condensed Gases. *Phys. Rev. Lett.*, 1999.

[16] D. J. McCarron, H.W. Cho, D. L. Jenkin, M. P. Koppinger, and S. L. Cornish. Dual-species Bose-Einstein condensate of ^{8}7Rb and ^{1}33Cs. *Phys. Rev. A*, 84 (011603), 2011.

[17] E. A. Cornell, D. S. Hall, M. R. MAtthews, and C. E. Wieman. Having It Both Ways: Distinguishable Yet Phase-Coherent Mixtures of Bose-Einstein Condensates. *Journal of Low Temperature Physics*, 113(314), 1998.

[18] Christopher Ticknor. The dispersion relation and excitation character of a two component Bose-Einstein Condensate. *Phys. Rev. Lett.*, 1(1403.3068), 2014.

[19] Peter Mason and Amandine Aftalion. Classification of the ground states and topological defects in a rotating two-component Bose-Einstein Condensate. *Phys. Rev. A*, 84(033611), 2011.

[20] R. A. Barankov. Boundary of two mixed Bose-Einstein Condensates. *Phys. Rev. A*, 66(013612), 2002.

[21] Peter Mason. Ground state of a two-component condensate in a harmonic plus Gaussian trap. *Eur. Phys. J. B*, 86(453), 2013.

[22] E. Timmermans. Phase Separation of Bose- Einstein Condensates. *Phys. Rev. Lett.*, 81(26), 1998.

[23] Minoru Eto, Kenichi Kasamatsu, Muneto Nitta, Hiromitshu Takeuchi, and Makoto Tsubota. Interaction of half-quantized vortices in teo-component Bose-Einstein condensates. *Phys. Rev. A*, 83(063603), 2011.

[24] Appendix B.

[25] John H. Matthews and Kurtis D. Fink. *Numerical Methods using Matlab*. 2004.

[26] F. Dalfovo, L. Pitaevskii, and S. Stringari. Order parameter at the boundary of a trapped Bose gas. *Phys. Rev. A*, 54(5), 1996.

[27] F. Dalfovo, L. Pitaevskii, and S. Stringari. The Condensate Wave Function of a Trapped Atomic Gas. *Journal of Research of the National Institute of Standards and Technology*, 101(4), 1996.

[28] Juan Polo and Swati Sridhar et al; in preparation.

[29] Francesco V. Pepe, Paolo Facchi, Giuseppe Florio, and Saverio Pascazio. Domain wall suppression in trapped mixtures of Bose-Einstein condensates. (67.85.Hj, 67.85.Bc, 03.75.Mn), 2012.